

Embryology and early development of the eye and adnexa

- Introduction
- General embryology
- Ocular embryology: general introduction
- Periocular mesenchyme is derived from a mixture of neural crest and mesoderm
- The neural retina and retinal pigment epithelium are derived from neuroepithelium
- Optic nerve and disk development
- Development of the fibrous coat of the eye
- Development of the intraocular contents
- Development of the uveal tract
- Development of the anterior chamber angle and aqueous outflow pathways
- Development of the extraocular muscles
- Development of the eyes and surrounding structures is influenced by the pattern of development of the skull, pharyngeal arches and face

Introduction

This chapter aims to provide an embryological basis for understanding the anatomy of the eye and adnexa. Basic embryological and developmental events from the earliest formation of diverticula in the forebrain at the beginning of the fourth week to the maturation of the various components of the eye in fetal life that influence the final differentiation and functional specialization of the adult eye are described. The contribution of the neural ectoderm, surface ectoderm and periocular mesenchyme to the final configuration of the adult eye and surrounding tissues of the head is emphasized. The cellular interaction and influence of gene expression and transcription factors in determining

cell fate will be outlined and examples are given where disruption of gene function underlies disturbances in these embryological events and the interactive processes between the various embryonic tissue and cell types lead to congenital abnormalities in humans.

General embryology

Before considering eye development, which commences in the fourth week, it may be useful for some readers to review the embryological events of the first 3 weeks following fertilization (see eFig. 2-1 and Video 2-1).

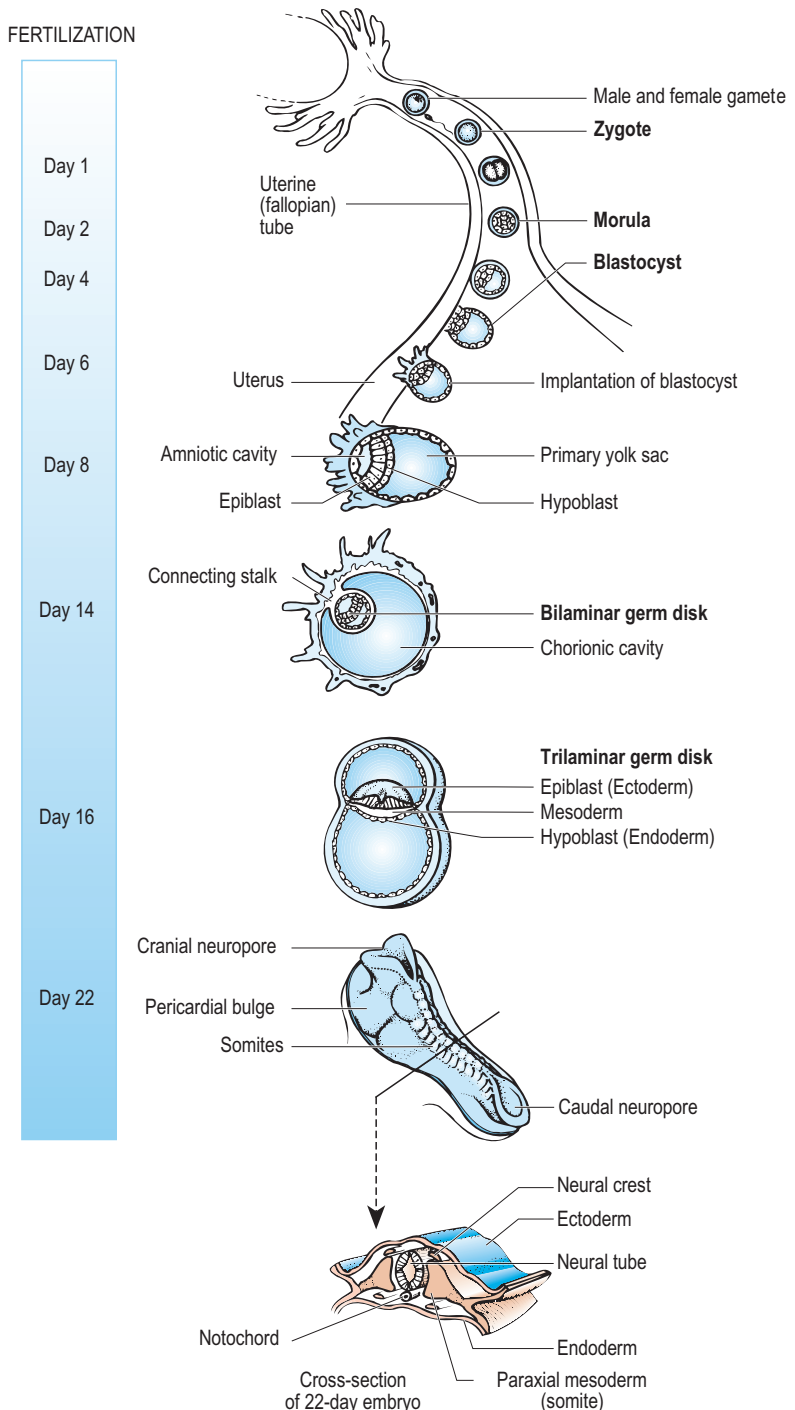
Additional content available at <https://expertconsult.inkling.com/>



Ocular embryology: general introduction

Although eye development can be considered from an embryological perspective to commence around day 22, when the *optic sulci* (optic primordium) appear as shallow grooves or pits in the inner aspect of the neural plate or neural folds (Fig. 2-1A) and the embryo is around 2 mm in length with eight somites, the group of cells that constitute the eye primordium or eye field have already begun to express a set of ‘eye field transcription factors’ (EFTFs) that are highly conserved in our evolutionary ancestry (see below). The neural folds have commenced fusion to form the neural tube but the optic sulci form before they have completed their closure rostrally and caudally. When the folds in this area fuse shortly afterwards they give rise to the future *diencephalon* region of the *prosencephalic (forebrain)* vesicle. The optic sulci evaginate to form hollow diverticulae – the *optic vesicles* (Fig. 2-1B).

By about day 25 (20-somite stage) the hollow optic vesicles enlarge and become ensheathed by mesenchymal cells, except at the apex of the vesicle, which is



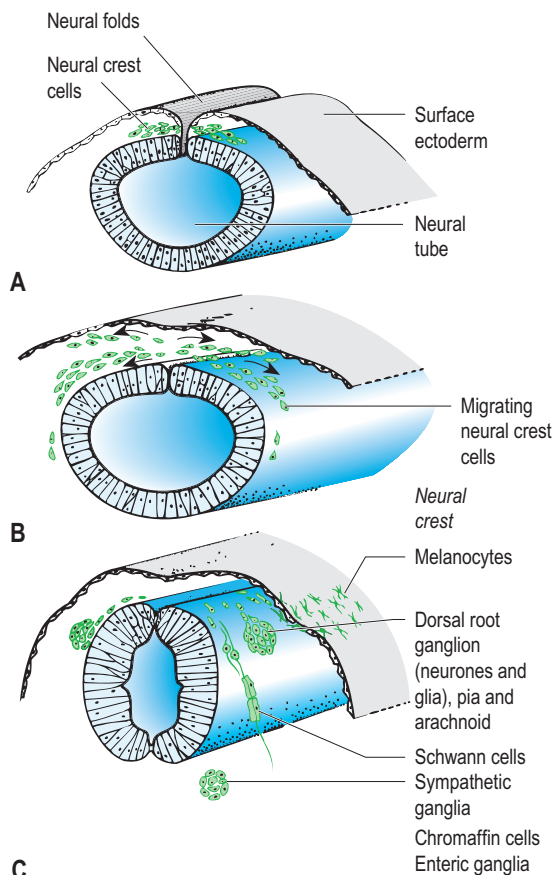
eFIGURE 2-1 Summary of embryological events occurring in the first 3 weeks following fertilization.

The male and female *gametes* unite at fertilization, which generally occurs within the oviduct or uterine tube, to form the *zygote*. The newly formed diploid cell undergoes *cleavage* as it travels towards the uterus. Within the solid mass of cells (30-cell stage) or *morula*, the *blastocyst cavity* appears. The earliest *differentiation* of the embryo occurs around this stage when two groups of cells are formed: a peripheral *outer cell mass* or *trophoblast* and a central *inner cell mass* or *embryoblast*. The *embryoblast* will give rise to the embryo proper and some of its attached membranes. By day 5 or 6 the embryo is a hollow spheroid of around 100 cells, known as the *blastocyst*. The *embryoblast* is evident as a heterogeneous collection of cells at one pole of the blastocyst; the remainder forms the *trophoblast*. This differentiates into the *syncytiotrophoblast* and the *cytotrophoblast*, which contribute to the fetal component of the placenta. Around this time the blastocyst enters the uterus and commences implantation into its rich endometrial lining.

At the beginning of the second week two cavities appear within the embryoblast. One forms the *amniotic cavity*, lined by epiblast cells, while the other forms the *yolk sac*, lined by cells derived from the hypoblast. Where the two cavities impinge there is a double discoid layer of cells, the *epiblast* or *primary ectoderm* and the *hypoblast* or *primary endoderm*. These two flat disks of cells constitute the *bilaminar germ disk*, which will develop into the embryo proper.

The third week of development commences with formation of the *primitive streak* and *primitive knot* or node at the caudal (tail) end of the epiblast. It is here that epiblast cells detach and migrate laterally and cranially into the potential space between the epiblast and the hypoblast to form the *intraembryonic mesoderm* or third germ layer. Some of the epiblast cells also replace the original hypoblast to form the *definitive* or *secondary hypoblast*. The epiblast is now known as the *ectoderm*. Formation of the primitive streak establishes the craniocaudal axis and bilateral symmetry of the future embryo. The formation of the *notochord* by budding from the primitive knot induces the formation of the *neural plate*. A series of *paraxial mesodermal* condensations or *somites* form along each side of the neural plate as it folds to form the *neural tube*, the precursor of the central nervous system ([eFig. 2-1](#)). A special group of cells, the *neural crest* cells, detach or delaminate from the margins of the neural folds and undergo extensive migration throughout the embryo where they differentiate into a remarkable variety of cells and tissues ([eFig. 2-2](#)). Derivatives of trunk neural crest cells are shown in [eFigure 2-2](#). Derivatives in the head are more extensive.

Anatomically, the human embryo is described as being in the prone (face-down) position. The terms dorsal and ventral correspond to posterior and anterior in the adult. The terms rostral and caudal correspond to superior (head end) and inferior (tail end).



eFIGURE 2-2 Diagrammatic summary of the origin (**A**), migratory pathway (**B**), and derivatives (**C**) of neural crest cells in the trunk.

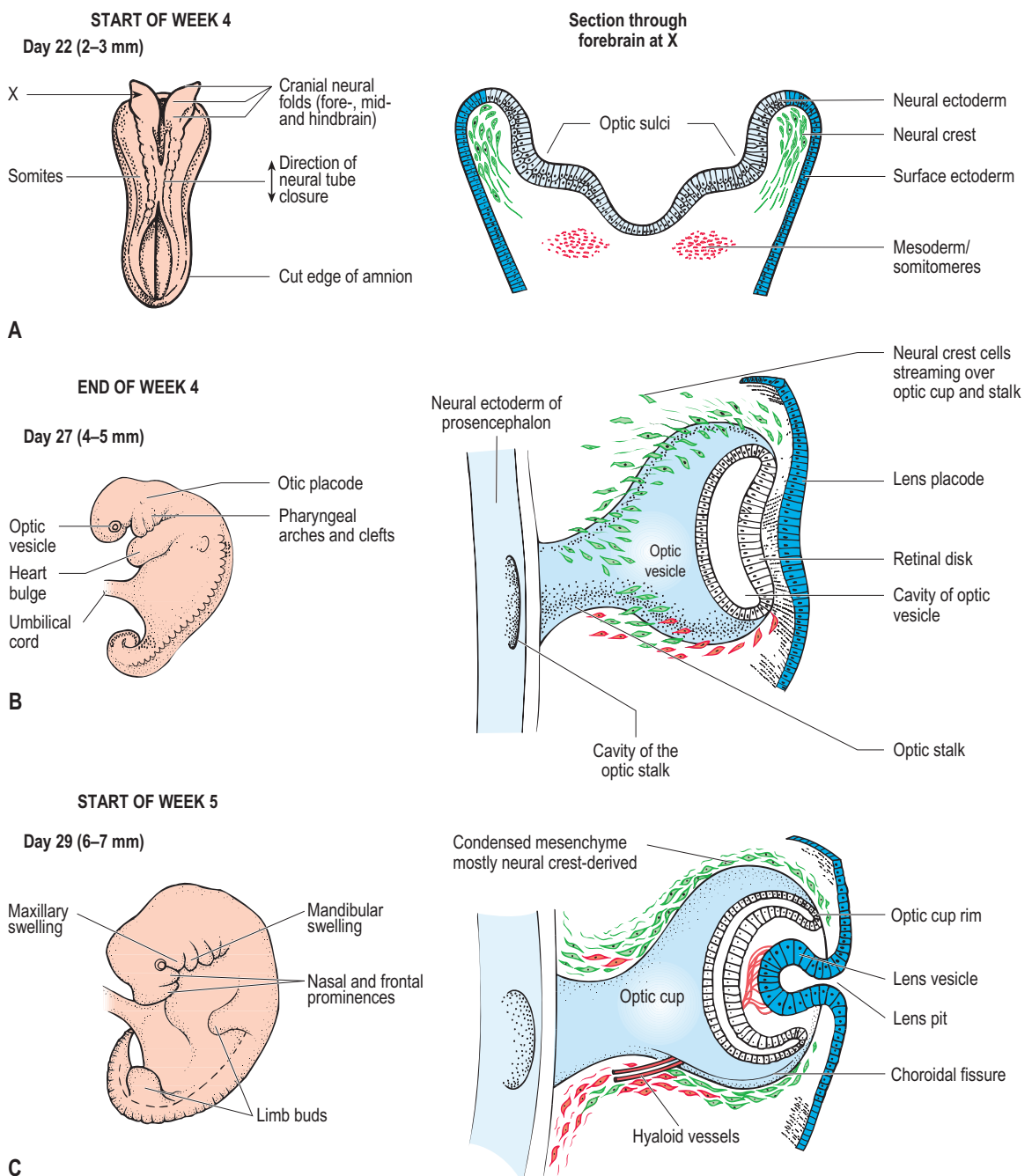
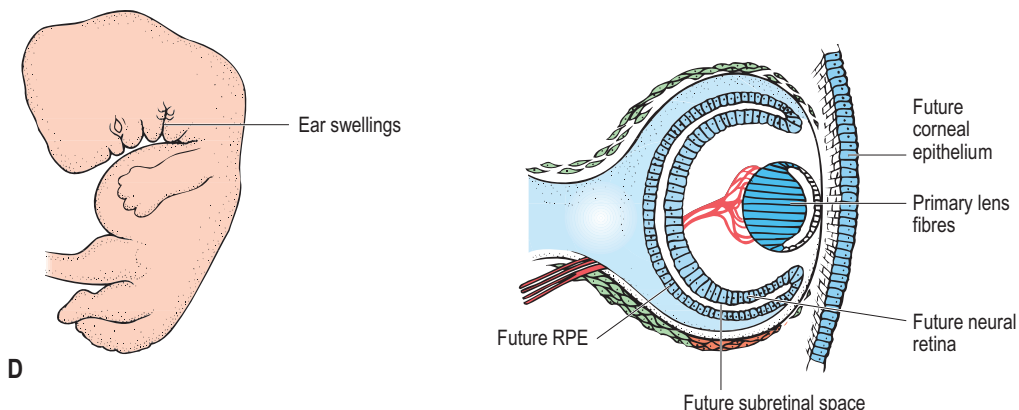


FIGURE 2-1 Diagrammatic summary of ocular embryonic development from day 22 to week 8. The external appearance of the whole embryo at the equivalent period is shown on the left. The various ‘germ layers’ are colour-coded to illustrate their origin and final contribution to the eye and periocular tissues.

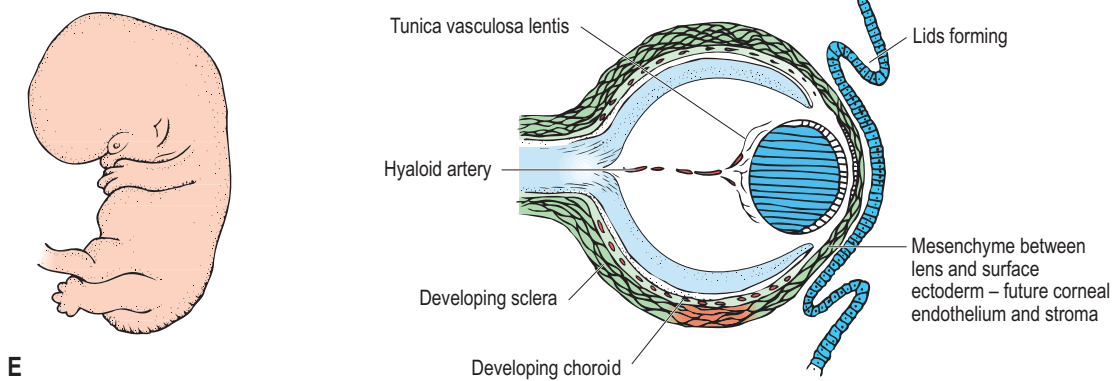
START OF WEEK 6

Day 37 (8–11 mm)



START OF WEEK 7

Day 44 (13–17 mm)



WEEK 8 (20–30 mm)

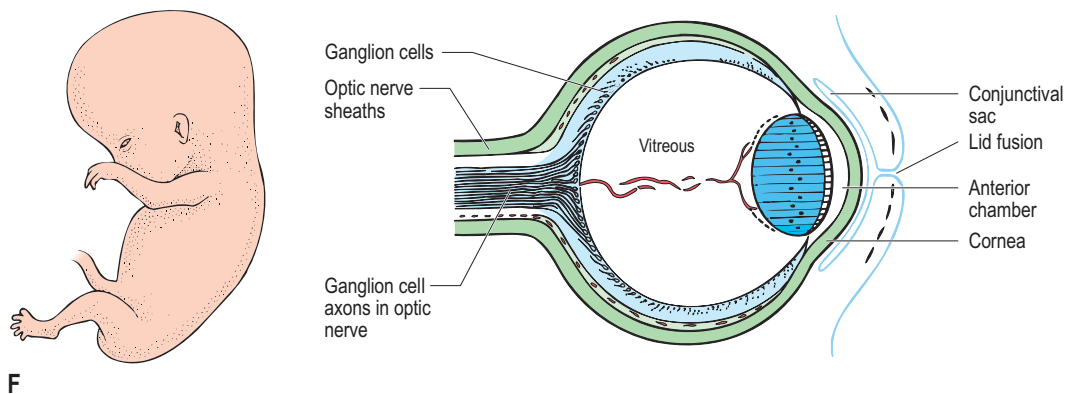
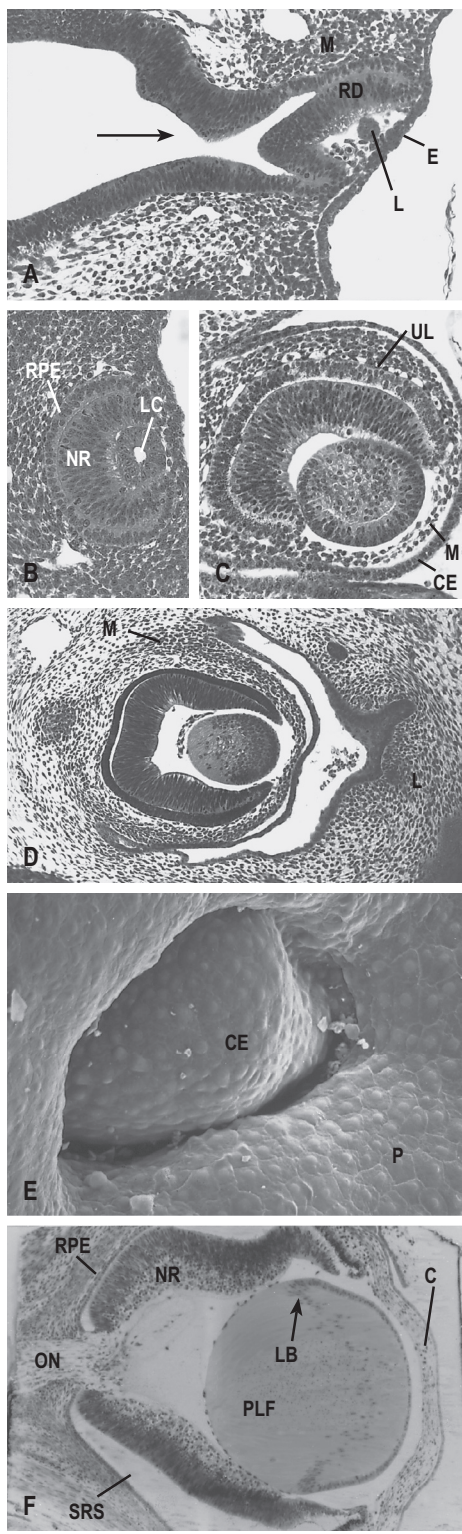


FIGURE 2-1, cont'd



closely apposed to the *surface ectoderm* on the lateral aspect of the developing head. This mesenchyme is derived from a mixture of cephalic neural crest and both para-axial and prechordal mesoderm (see eBox 2-1).

A disk-shaped thickening of the neural ectoderm, the *retinal disk* (future neural retina), lies beneath a localized thickening of the surface ectoderm, which on day 27 is recognizable as the *lens placode* (Fig. 2-1B). Formation of the lens placode directly adjacent to the underlying neural ectoderm is regarded as one of the best examples of *induction* in developmental biology. Lens placode formation coincides with the formation of a constriction in the optic vesicle at its attachment to the wall of the forebrain to form the *optic stalk*. The *cavity of the optic vesicle* or *optic ventricle* (future subretinal space) is continuous, via the lumen in the optic stalk, with the future third ventricle (Figs 2-1B and 2-2A).

The single-layered spheroidal *optic vesicle* undergoes active invagination to fold in on itself creating two ‘nested’ layers of the goblet-shaped *optic cup*. The distal part of the optic vesicle becomes the inner layer or *presumptive neural retina*, whereas the proximal part of the optic vesicle becomes the outer layer of the

FIGURE 2-2 Histological and scanning electron micrographs of early mammalian eye development (chronological sequence A–F). (A) The cavity of the optic vesicle is clearly in continuity via the cavity of the optic stalk with the forebrain ventricle (arrow). M, mesenchyme condensation; E, surface ectoderm/periderm; L, lens vesicle; RD retinal disk. (B) The lens vesicle, containing a distinct lens cavity (LC), fills the optic cup, which consists of two layers, an outer retinal pigment epithelium (RPE) and neural retina (NR). (C) Mesenchyme has condensed around the optic cup and migrated over the cup margin to form the future corneal endothelium/stroma (M) beneath the surface ectoderm-derived corneal epithelium (CE). Beneath the RPE the vascular mesenchyme has already formed a distinct row of vessels, the uveocapillary lamina (UL) or presumptive choroid. (D) Pigment is identifiable in the RPE layer. The lentoretinal space contains vascular mesenchyme. The mesenchyme (M) around the developing eye has now formed two layers, an outer dense avascular layer (future sclera) and an inner vascular layer (future choroid). Beneath the newly formed lids (L) lies the conjunctival sac. (E) Scanning electron micrograph of the embryonic corneal epithelial surface (CE) and periderm (P) just before lid closure. (F) Late embryonic eye with well-developed cornea (C), large lens consisting of primary lens fibres (PLF) whose nuclei form the lens bow (LB). The neural retina (NR) is artefactually detached from the RPE, producing a large subretinal space (SRS). Axons have commenced migration along the optic nerve (ON). Original magnifications: A, $\times 120$; B, $\times 180$; C, $\times 160$; D, $\times 55$; E, $\times 100$; F, $\times 65$. (From McMenamin and Krause, 1993, with permission.)

eBox 2-1**Mesenchyme**

This is a term used to describe the tissue occupying the embryo between the surface ectoderm (and derivatives such as neuroectoderm) and the endoderm-derived epithelial layers. It is a loose tissue consisting of stellate amoeboid mesenchymal cells embedded in a matrix rich in glycosaminoglycans. Mesenchymal cells may be derived from several sources, namely mesoderm (dermatome or sclerotome component of the somites or lateral plate mesoderm) or neural crest. Thus, the descriptive term 'mesenchyme' does not imply an origin from any particular embryonic germ layer.

optic cup, namely the presumptive retinal pigment epithelium. The thickened retinal disk at the tip or distal part of the vesicle (Fig. 2-1B,C) and the ectoderm-derived lens placode invaginate via a combination of differential growth (cell elongation and mitosis) and buckling to form the dorsal hemisphere of the optic cup and the lens vesicle. This combined invagination may also be aided by temporary fine cellular bridges between the lens placode and the retinal disk and is mediated by the extracellular matrix protein fibronectin-1 (*Fn1*), whose extent and circumferential limit beneath the lens placode is regulated by *Pax6* expression (Fig. 2-3). The active growth of the optic cup is not uniform around the circumference, which leads to the development of a groove at the distal and ventral aspect where the margins form the *choroidal* or *optic fissure*. By day 29 invagination of the retinal disk and lens placode is almost complete (Figs 2-1C and 2-2A). A small *lens pit* can be identified just before the surface ectoderm seals over the site of lens placode invagination. By the start of day 36 the *lens vesicle* separates from the surface ectoderm. The lens epithelial cells enclose the *lens cavity* and are surrounded externally by a basal lamina, which will form the future *lens capsule*. The longitudinal groove of the optic fissure, which extends into the optic stalk, acts as a temporary deficiency in the expanding and invaginating cup through which vascular mesenchyme and a branch of the ophthalmic artery, the *hyaloid artery*, become incorporated into the fissure and thus gain access to the lentoretinal space. By the end of the sixth week the growing edges of the choroidal or optic fissure meet and fuse; thus the hyaloid vessels and associated mesenchyme become situated in the centre of the optic stalk and form the future central retinal artery and vein (Fig. 2-1D,E). The fusion or closure of the optic fissure commences at the mid-portion of the optic stalk and continues both proximally and distally. It is completed distally at the margins of the optic cup that will eventually form the pupil.

Following separation of the lens vesicle from the surface ectoderm this layer regenerates and closes the lens pit and ectodermal layer in this region forms the future corneal epithelium (Fig. 2-2E). Around this time (day 39) a 'wave' of mesenchyme passes over the rim of the optic cup, directly beneath the surface ectoderm (Figs 2-1D,E and 2-2C,D). The

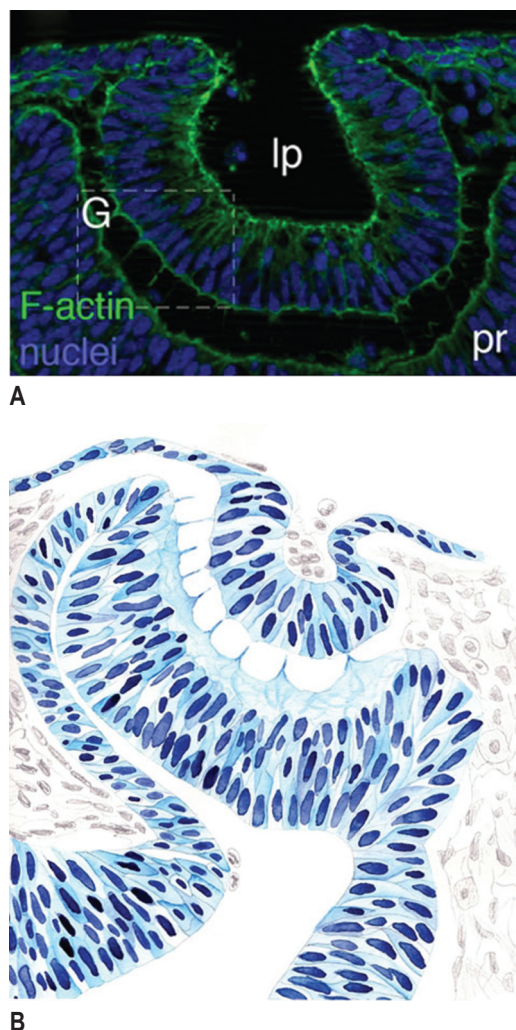


FIGURE 2-3 Transient, F-actin-filled processes connect lens and retina during lens pit-optic cup invagination in the mouse eye (sections from cytoplasmic protrusions interepithelial processes containing filamentous actin (F-actin, green) are clearly seen between the lens and future retina from E9.5 to E11.0 (embryonic days/post-conception). Equivalent interepithelial processes were described in the early human eye many years ago by Ida Mann. Ip, lens pit; pr, presumptive retina. Scale bars: 20 µm. Nuclear staining (Hoechst 33258, blue). (Part A reproduced from Chauhan et al., 2009, with permission; Part B redrawn from Mann, 1928)

cells in the first of the three waves of mesenchyme, which lie posteriorly closest to the lens, become flattened and form apicolateral contacts. These contacts become continuous bands of junctional complexes and thus form an endothelium. The other

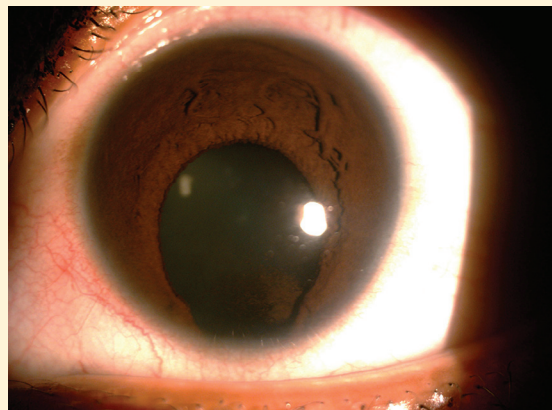
BOX 2-1 CLINICAL CORRELATES

Coloboma

The word coloboma ('a mutilation') in clinical practice is the term used to describe a defect in the inferonasal quadrant in the iris, ciliary body or choroid. Colobomas are usually sporadic and bilateral and do not lead to significant complications. They are the result of a failure of closure of the (inferonasal) optic fissure. The consequence is an interference with the normal induction and formation of uveal tissues. A coloboma of the iris appears as an *inferonasal defect* in the stroma, the smooth muscle and the pigment epithelium whereas a ciliary body coloboma is characterized by absence of ciliary processes and presence of a diminutive muscle. The adjacent lens is indented, owing to a failure of formation of the zonular fibres. In the colobomas associated with complex malformations and abnormalities (e.g. trisomy) there may be an ingrowth of mesodermal tissue into the retrobulbar space with formation of fat and cartilage.



Colobomas involving the retina may be large and may extend to the disk. In the retina adjacent to the coloboma, proliferation of neuroblastic tissue leads to the formation of rosettes. The retinal pigment epithelium and Bruch's membrane and choroidal tissue are absent at the site of the coloboma, although the underlying sclera is normal. In many cases of retinal coloboma there is glial and vascular ingrowth from the retina across the bed of the coloboma. Colobomas have been described in association with mutations in the *CHD7* gene (see Table 2-1). Mutations in the *CHD7* gene are found in approximately 60–65% of individuals with CHARGE syndrome (*Coloboma, Heart disease, Atresia choanae, Retardation of growth and/or development, Genital hypoplasia, Ear malformation*). Most mutations lead to the production of an abnormally short, non-functional *CHD7* protein, which appears to disrupt chromatin remodelling and the regulation of gene expression.



waves of mesenchyme will form the remainder of the cornea, iris stroma and iridocorneal angle mesenchyme.

By the end of the embryonic period (defined as the end of week 8 in humans) the retina can be clearly differentiated into a thin outer layer, which will form the *retinal pigment epithelium* (RPE) and a much thicker inner *neural retina* (Figs 2-1F and 2-2F). These two layers are separated by a narrow *intraretinal or subretinal space*, the remains of the almost obliterated ventricular cavity of the optic vesicle. Melanin first appears in the RPE around 5 weeks (Fig. 2-2C,D) and is visible on external examination of embryos of this gestational age. The neural retina commences its centrifugal

differentiation into an *inner* and *outer neuroblastic layer* near its continuity with the optic stalk. The lens cavity disappears as the posterior cells elongate to form the *primary lens fibres* (Figs 2-1D and 2-2D). Mesenchyme, mostly derived from neural crest cells, condenses around the external surface of the optic cup. The innermost layer of this mesenchyme is loose and highly vascular and will form the *choroid* (uveocapillary lamina) (Fig. 2-2C,D). It lies adjacent to a distinct basement membrane formed by the RPE, which is continuous with a similar membrane around the forebrain. Indeed, the choroid is homologous in its embryonic origin with the *pia mater* and *arachnoid* investing the brain. The outer layer of the condensed

TABLE 2-1 Critical genes in ocular development

| Mouse gene | Human gene | Expression pattern | Ocular defects in mouse mutants | Ocular defects in humans with known mutations in related gene |
|-----------------------------|-----------------------------|--|---|--|
| <i>Sox1, Sox 2, Sox3</i> | <i>SOX1, SOX2, SOX3</i> | Central nervous system, sensory placodes, <i>Sox2</i> in anterior neural ectoderm and lens placode | Micro-ophthalmia, cataract | Anophthalmia |
| <i>Otx2</i> | <i>OTX2</i> | Anterior neural ectoderm Future forebrain | | Range of phenotypes from bilateral anophthalmia to retinal dystrophy |
| <i>Rax</i> | <i>RAX</i> | Anterior neural plate, optic vesicle, developing retina, photoreceptors | Eyeless | Anophthalmia |
| <i>Pax-6</i> | <i>PAX6</i> | Anterior neural plate, optic sulcus/cup and stalk Surface ectoderm (future lens and corneal/conjunctival epithelium) Weakly expressed in mesenchymal cells | Micro-ophthalmia, cataract, hypoplastic iris, incomplete separation of cornea and iris, corneal defects | Anophthalmia, anterior segment dysgenesis, congenital glaucoma, Peters' anomaly, Axenfeld-Rieger syndrome (aniridia) |
| <i>Six3</i> <i>Pitx3</i> | <i>SIX3</i> <i>PITX3</i> | Presumptive eye field Developing lens vesicle | Lack of neural retina Persistent lens stalk, malformed lens | Holoprosencephaly Congenital cataract, leucoma, Peters' anomaly |
| <i>Chd7</i> | <i>CHD7</i> | Neuroectoderm, lens vesicle | CHARGE-like features, keratoconjunctivitis sicca | CHARGE syndrome (see Box 2-1) |
| <i>Maf</i> | <i>MAF</i> | Lens placode, lens vesicle, primary lens fibres (transcription factors for α -crystallin gene along with <i>Sox1</i>) | Failure of lens fibres to elongate, lens vesicle fails to separate from surface ectoderm | Defects in lens, cornea and iris (coloboma), Peters' anomaly |
| <i>Foxe3</i> | <i>FOXE3</i> | Lens placode | Failure of lens to separate from surface ectoderm | Peters' anomaly, posterior embryotoxon, cataract |
| <i>Pitx2 Fox1</i> | <i>PITX2 FOXC1</i> | Periocular mesenchyme (presumptive cornea, eyelids, trabecular meshwork, extraocular muscle) | Anterior segment abnormalities | Iridogoniodysgenesis, Axenfeld-Rieger syndrome, 50% develop juvenile glaucoma |
| <i>Crya, Cryb, Cryg</i> | <i>CRYA, CRYB, CRYG</i> | Lens | Various forms of cataract | Various forms of cataract |

mesenchyme will form the *sclera*, which is homologous to, and indeed continuous with, the dura mater around the optic nerve and brain posteriorly.

In the eighth and last week of the embryonic period (Figs 2-1F and 2-2F), ganglion cell axons grow from the inner retina towards the optic stalk. The axons travel within the stalk towards the brain, thus forming the optic nerve. Other major landmarks in development occurring in the eighth week include formation of secondary lens fibres, lens sutures and the secondary vitreous.

In summary, by the end of the embryonic period the eye comprises a double-layered neural ectoderm-derived optic cup containing a surface ectoderm-derived lens, both enveloped by condensed mesenchyme comprising a dense outer layer (the bulk of the future cornea and sclera) and an inner vascular layer which will form the choroid and stroma of the iris and ciliary body. At this stage the human embryo is 30 mm in length (crown–rump length) and the developing eye is 1.5–2.0 mm in diameter (Figs 2-1F and 2-2F).

GENETIC REGULATION OF EYE DEVELOPMENT

It is now clear that *epigenetic development*, the process by which invertebrates and vertebrates develop their definitive characteristics through the gradual alteration of simpler precursors, is regulated by *cascades of gene expression*. That is, early acting regulatory genes initiate developmental processes and induce the expression of '*downstream*' genes, which may subsequently lead to expression of further genes and so on until genes encoding actual structural and functional characteristics of specific cells and tissues are activated. There is overwhelming evidence that these cascades have been conserved throughout evolution from insects to fish to mammals. The *Drosophila*, or fruit fly, zebra fish and mouse are the most intensively studied experimental species in each respective group and recent research has shed light on some of the critical genes in ocular development, some of which have been remarkably conserved in evolution. The clues from animal studies have aided clinical geneticists to screen the DNA from patients with abnormalities and have helped reveal how mutations in single genes can cause congenital abnormalities, and the eye has provided science with some of the more elegant

examples of the relevance of such genetic studies (Table 2-1) (see Ch. 3).

The basic body plan of all animal embryos is initially established by a class of regulatory genes called *selector* or *switch genes* which, like the *maternal effect genes* of the fruit fly, establish longitudinal or antero-posterior (head–tail), dorsoventral and left–right axes. A further class of genes, the *zygotic genes*, which includes *segmentation genes*, is switched on later, after the maternal effect genes. The changes induced by the segmentation genes cause the expression of another class of selector genes, the *homeotic genes*, which encode a region of DNA called a *homeobox* (termed *Hox genes*). These subsequently regulate many downstream genes and thus act as *master control genes*.

Hox gene activation plays a critical role in the differentiation of what initially appear as identical segments in the embryo (induced by earlier expression of segmentation genes) into, for example, cervical, thoracic, abdominal and sacral regions as well as the segmentation of the head and neck, particularly the pharyngeal arches and subdivision of the brain.

Paired-box (Pax) genes encode transcription factors involved in the regulation of several aspects of vertebrate and non-vertebrate early development and, as such, are also considered as '*master control genes*'. In vertebrates two *Pax* genes, *Pax-6* and *Pax-2*, are important eye field transcription factors.

EYE FIELD TRANSCRIPTION FACTORS

In mammals (and one must appreciate that much of this research is performed in mice) the eye field transcription factors (EFTFs) include *Pax-6*, *Rax*, *Six3* and *Lhx2* and these are expressed in an overlapping fashion in the anterior neural plate or future forebrain at the paired sites that define the site of the eye primordium or eye field (Fig. 2-4). There is evidence that *Otx2*, a transcription factor essential for forebrain development, may cooperate with *SOX2*, a neural ectoderm transcription factor, to progressively activate *Rax* expression in the eye field, which may in turn activate *Pax-6*, *Rax*, *Six3* and *Lhx2*. Evidence of the importance of these genetic transcription factors in early developmental events can be seen by considering the effects of mutations in both mouse models and humans (see Table 2.1).

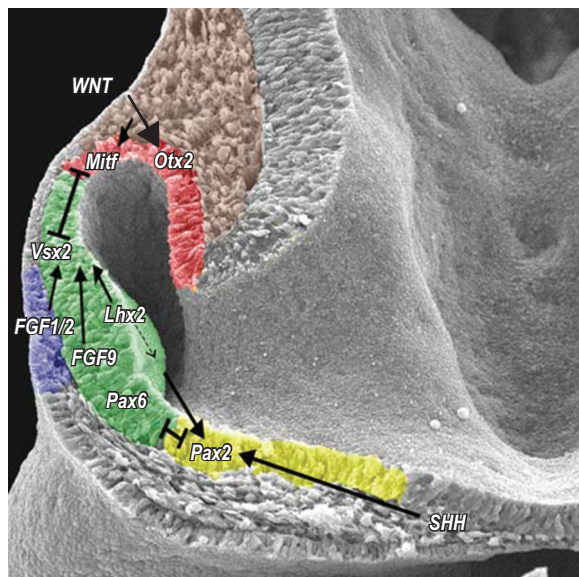


FIGURE 2-4 Signalling networks establish boundaries in the optic vesicle. Dorsal is to the top, and distal is to the left (note the cavity of the optic stalk communicating with the forebrain vesicle (left)). The optic vesicle is regionalized into prospective RPE (red, dorsal), neural retina (green, central) and optic stalk (yellow, ventral). Extracellular signals organize the optic vesicle in part through the activation of transcription factors that specify the tissue type in which they are expressed. These transcription factors cell-intrinsically regulate optic vesicle organization through mutual repression of one another. The lens placode, which expresses fibroblast growth factor (FGF) ligands important for neural retinal specification, is shown in blue. (Reproduced from Heavner W, Pevny L. Eye development and retinogenesis. Cold Spring Harb Perspect Biol. 2012;4:a008391 with permission.)

The primordial eye field is initially one region of anterior neural ectoderm that has two hemispheres that later split into two respective fields, a left and a right, and at least two molecules (*sonic hedgehog* (*Shh*) and *Six3*) are involved in this early morphogenesis, which, if disrupted, leads to a failure in the splitting, and thus to cyclopia or a single midline eye.

Pax-6 is expressed in the anterior neuroepithelium and lens placode-forming epithelium. Thus it appears that the gene defines a field of cells *competent to differentiate into eye tissues* (neural retina, retinal pigment epithelium, iris epithelium, ciliary body epithelium, lens and corneal epithelium). It also appears to be required to *maintain growth and proliferation* of cells in the optic vesicle (and other regions of the central nervous system). Mice with mutations in *Lhx2* can

generate optic vesicles but never form optic cups and it appears as if both this transcription factor and *Pax-6* are needed to form a proper eye cup and together induce *Six3* in the optic vesicle, which is essential for retinal differentiation. The boundaries between the parts of the optic vesicle that ultimately differentiate into neural retina, RPE and optic stalk are predetermined by the differential expression of cell signalling pathways along the dorsoventral and proximal-distal axes, which are in turn regulated by transcription factors (Fig. 2-4). For example, a mutually antagonistic relationship exists between expression of *Pax-2* and *Pax-6*. *Pax-2* is largely restricted to the future optic stalks on the ventral aspect where it appears to be necessary for successful closure of the *choroid fissure*, whereas *Pax-6* is expressed more dorsally and is more involved with formation of the RPE and neural retina. These cell-intrinsic signalling pathways are not the only factors that determine the fate of cells or patterning in the optic vesicle. There are further extrinsic factors including members of the transforming growth factor- β (TGF- β), fibroblast growth factor (FGF) and Wnt families and *Shh* that signal to functionally compartmentalize the optic vesicle. For example, ectopic expression of FGF9 in the presumptive RPE promotes neural retina formation and inactivation of canonical Wnt signalling in the future RPE causes it to transdifferentiate into neural retina.

Periorcular mesenchyme is derived from a mixture of neural crest and mesoderm

For many years it was widely held that the middle germ layer, the *mesoderm*, gave rise to most of the mesenchyme and its derivatives in the head and neck region in a similar manner to the pattern of differentiation in the trunk (see eFig. 2-2).

A large body of experimental evidence from avian and mammalian studies has now shown that mesenchyme in the head region is derived from two sources, neural crest (*mesectoderm*) and mesoderm. Neural crest cells originate at the neuroectoderm-surface ectoderm junction of the fore-, mid- and hindbrain regions before fusion of the neural folds. They migrate ventrally into the pharyngeal arches and rostrally around the forebrain and developing optic cup and into the facial region in a highly ordered manner,

BOX 2-2 CLINICAL CORRELATES**Malformations of the neural tube and optic vesicle and genetic factors**

These occur in the first month of embryonic life and include:

- **Anophthalmia.** Extremely rare and the result of a failure of formation of the optic vesicle. The orbits do not contain ocular tissue, but the extraocular muscles (mesoderm) and lacrimal gland (ectoderm) are present. Mutations in the *RAX* and *SOX2* genes have been associated with anophthalmia (Table 2-1).
- **Nanophthalmia and microphthalmia** Formation of the optic vesicle without proper subsequent development produces a rudimentary eye in the orbit – nanophthalmia (or dwarf eye). In microphthalmia there is a small but recognizable eye that contains recognizable elements, e.g. lens, choroid and retina. The mouse mutant small eye (*Sey*) has a haploinsufficiency in *Pax-6*. Human mutations in one copy of *PAX6* have aniridia (iris abnormalities) and microphthalmia but homozygous loss causes anophthalmia. Mutations in *SOX2* can also cause microphthalmia.
- **Cyclopia** Mutations in *SHH* or *SIX3* result in midline defects including cyclopia.
- **Synophthalmia.** Fusion of the two eyes may result from a malformation of the mesenchymal tissue between the optic vesicles or faulty inductive processes. Only rarely is a single eye (cyclops) formed by this mechanism and in most cases there are two recognizable corneas and lenses, and identifiable parts of the iris and ciliary body. The midline sclera and uveal tissue may be absent and the optic nerve may be single or duplicate. This malformation may be associated with a deletion of chromosome 18.

guided in their migration by components of the extracellular matrix, such as fibronectin and glycosaminoglycans (Fig. 2-5). The pattern of appearance and migration of cranial neural crest is closely associated with the expression products of the *homeobox* (*Hox*) gene family within the rhombomeres of the hindbrain. In the face region, neural crest cells contribute significantly to mesenchyme-derived tissues, such as bone, cartilage, connective tissues, meninges and ocular and periocular connective tissues (which normally do not arise from trunk neural crest), as well as giving rise to the usual crest derivatives: melanocytes, dorsal root ganglia equivalents (sensory ganglia of V, VII, IX

and X) and parasympathetic ganglia (ciliary, otic, pterygopalatine and submandibular).

At the same time as cephalic neural crest cell migration commences, the optic stalks begin to constrict, thus creating a pathway between the stalk and surface ectoderm into which predominantly mesencephalic crest cells migrate. The migration of these cells ceases when they reach the choroid fissure on the ventral aspect of the optic cup (for further information see eBox 2-2).

 Paraxial mesoderm (somites and the less distinct rostrally situated somitomeres) forms most of the walls and floor of the brain case, all voluntary muscles of the craniofacial region (including extraocular muscles), all vascular endothelial cells, the dermis and connective tissues of the dorsal region of the head, and the meninges caudal to the prosencephalon. The seven rostrally situated somitomeres differentiate in a segmental manner within the pharyngeal arches and they play an important role in eye development by influencing neural crest cell migration and differentiation and by directly contributing to the periocular mesenchyme (Fig 2-6).

Thus, mesodermally derived mesenchyme contributes more to the periocular connective tissues than experimental studies in birds had previously suggested.

The neural retina and retinal pigment epithelium are derived from neuroepithelium

The thickened portion of the optic vesicle that invaginates, the *retinal disk*, is destined to differentiate into the *neural retina*, while the thinner outermost layer of the optic vesicle is destined to form the RPE. These layers are continuous at the optic cup margin, where a sharp transition in morphology is evident (Figs 2-1B,C and 2-2A–D). The *optic cup margin* will later be the site from which the neuroepithelial component of the iris and ciliary body will arise and ultimately form the *pupil margin*. Because of the invagination of the optic cup the apical aspect of the primitive neural retina comes to lie adjacent to the apical surface of the RPE, thereby obliterating the intraretinal space (Fig. 2-1C).

eBox 2-2***Experimental methods of mapping neural crest cell migration and fate***

The fate of neural crest cells from various regions of the neural plate has been mapped in birds (for reviews, see Noden, 1982, 1988; Creuzet et al., 2005); it has also been mapped in mouse and rat embryos (Erickson et al., 1989; Fukiishi and Morriss-Kay, 1992; Trainor and Tam, 1995). Avian experiments have used a variety of cell-tracing methods, including transplanted radiolabelled donor crest cells, chick-quail transplant chimeras and subsequent tracking of quail cells using natural nucleolus marker or anti-quail nuclear antigenic determinant (for review, see Creuzet et al., 2005).

Tracking the fate of neural crest cells in mammals has been aided by the production of mouse mutants with neural developmental anomalies and more recently by utilizing transgenic mice in which a transgene (bacterial *lac Z* 'reporter' gene which codes for β -galactosidase) is introduced into the mouse genome in a position where it will be co-expressed alongside proteins specific for the cell types under investigation, such as peripherin or retinoic acid receptor, which are expressed on neural crest cells during and after migration. The migration pathways of the cells carrying the transfected genome can thus be visualized with appropriate chemical substrates for bacterial β -galactosidase (Mendelson et al., 1994). Other techniques that are unveiling the destiny and differentiation of various cell types in embryonic development include micromanipulative cell grafting and labelling using fluorescent cell markers (Dil and DiO), *in situ* hybridization and chimeric and mosaic mouse models (Osumi-Yamashita et al., 1990; Trainor and Tam, 1995; Collinson et al., 2004) (see Fig. 2-6).

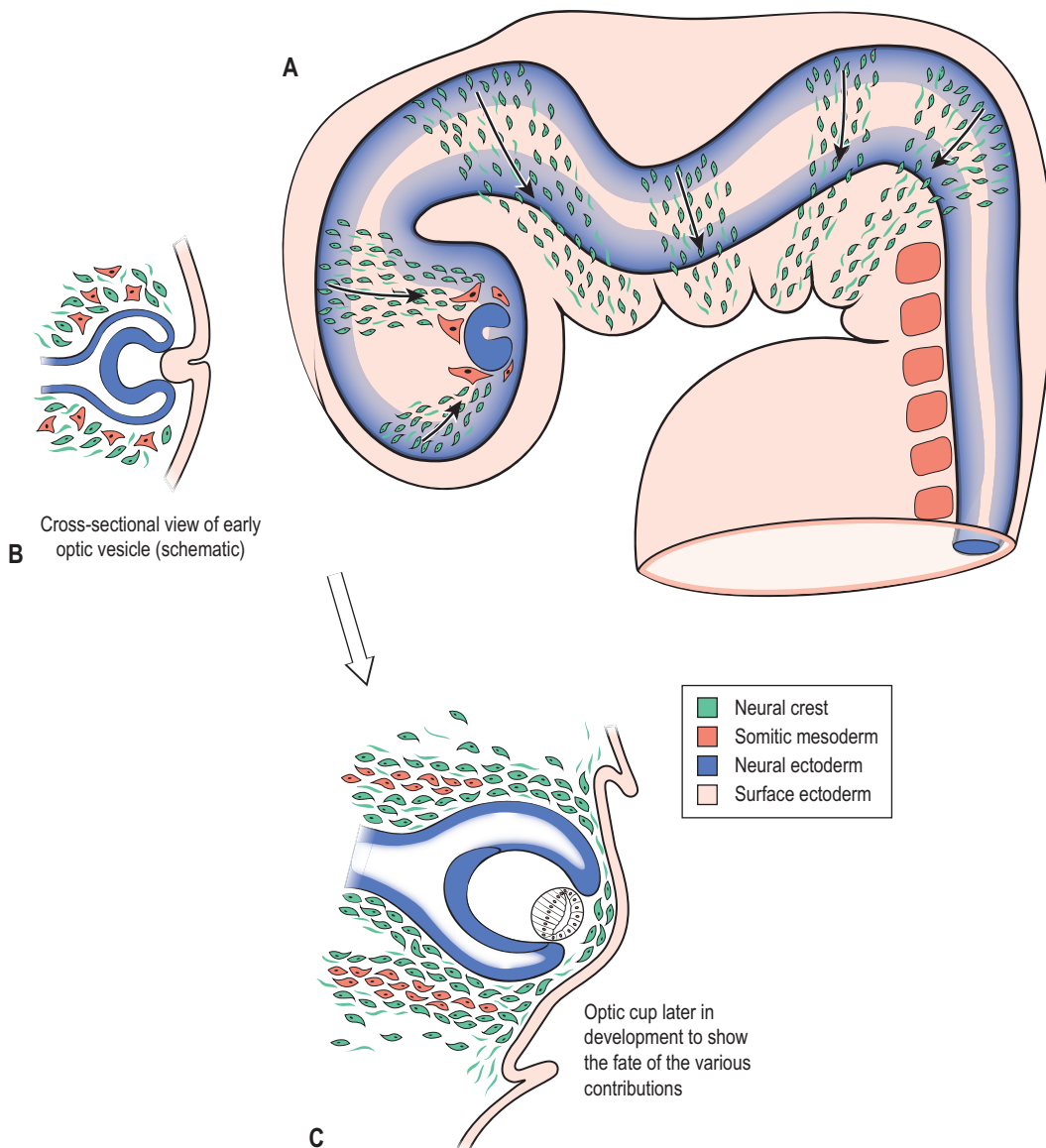


FIGURE 2-5 Diagrammatic summary of the interactions between surface ectoderm, neural ectoderm, neural crest and mesoderm early in development and their final contributions to the eye and periocular tissues.

Just as the ependymal cells that line the developing (and adult) ventricular spaces in the brain are ciliated, the apposing surfaces of the primitive neural retina and future RPE are also ciliated. The cilia of the neural retina are important later in development, in the formation of rods and cones. The cilia of the RPE degenerate.

AXES IN THE NEURAL RETINA

We now understand more clearly how the axes in the retina which are critical to establishing the pattern of retinotopic projection become organized during development. Mouse studies have shown that when the inner layer of the optic cup invaginates to form the neural retina it must establish three primary axes:

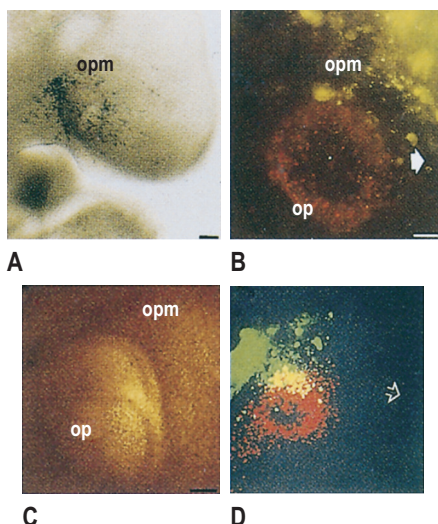


FIGURE 2-6 Colonization of the periocular mesenchyme (opm) by cells derived from somitomere I in the mouse embryo. In (A) the cells have been labelled with X-gal (blue) and in (B) with DiI (green fluorescence). In (B) the red cells are Dil-labelled neural crest cells. (C) A bright field view of the same specimen showing the orientation of the optic vesicle (op) and periocular mesenchyme (opm). (D) A confocal image showing the co-distribution of the two cell populations showing that neural crest cells are found in both the neural epithelium of the optic vesicle and in the surrounding mesenchyme where they share territory with somitomeric-derived mesenchyme (yellow indicates areas of overlapping distribution but not double-labelled cells). Arrow points rostrally. Bar, 500 µm. (Reproduced from Trainor and Tam, 1995, with permission.)

dorsoventral, nasal–temporal and anterior–posterior. In addition, the optic stalk must form inferiorly relative to these axes (Fig. 2-7). The signalling that is important in the dorsoventral axes are mediated through the *Pax-6* (highest expression dorsally) and *Pax-2* (highest expression ventrally) transcription factors in addition to the VAX family of homeodomain transcription factors. *Vax2*, in particular, has a steep ventral–dorsal gradient, whereas *Vax1* is expressed on the optic stalk. Naso-temporal patterning is regulated by the forkhead transcription factors *FOXD1* and *FOXG1* (Fig. 2-7).

RETINAL MORPHOGENESIS (Fig. 2-8)

The primitive neural retina consists of an *outer nuclear zone* and an *inner acellular or marginal zone*. The outer nuclear zone is homologous with the proliferative

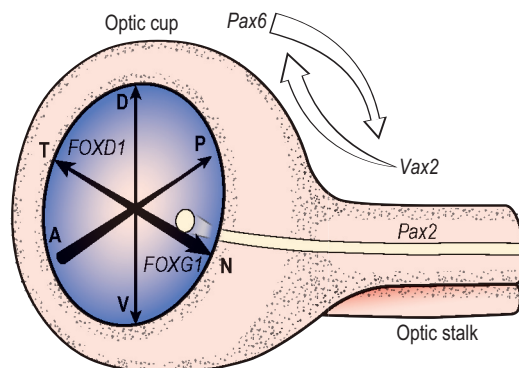


FIGURE 2-7 Regulation of the axes in the optic cup and optic stalk by differential expression of transcription factors which determine the regional specificity or fate of the retina along dorsal-ventral (D-V), naso-temporal (N-T) and antero-posterior (A-P) axes.

neuroepithelium of the neural tube. Both the inner and outer layers of the optic cup rest on their respective basal laminae: that of the inner layer becomes the *inner limiting membrane*, the outer is incorporated into *Bruch's membrane*. Differentiation of the retinal layers commences at the posterior pole and progresses in a centrifugal manner; thus a gradient of retinal differentiation can be seen within an individual eye. Miotic activity in the primitive neural retina is greatest in the outer part of the nuclear zone (Fig. 2-8A). Around 7 weeks of gestation (16–20 mm) newly formed cells migrate in a vitread direction into the marginal zone to form the *inner neuroblastic layer*. The outer nucleated zone is now referred to as the *outer neuroblastic layer* (Figs 2-8B and 2-9A). The two neuroblastic layers are separated by an acellular zone – the *transient layer of Chievitz*. The earliest differentiated cells, which form the inner neuroblastic layer, are future ganglion cells, Müller cells (radial glial) and amacrine cells. Elegant studies using chimeras and mosaic mouse models have revealed that clones of cells radiate in a vitread direction and, as the retina begins to stratify, proliferation and differentiation cells that have arisen from these original ‘clones’ appear as columns. Subsequently some cells disperse laterally.

The nerve fibre layer becomes identifiable on the inner aspect of the inner neuroblastic layer owing to growth of ganglion cell axons that converge towards the optic stalk. A zone where the processes of cells from the inner neuroblastic layer intermingle (the

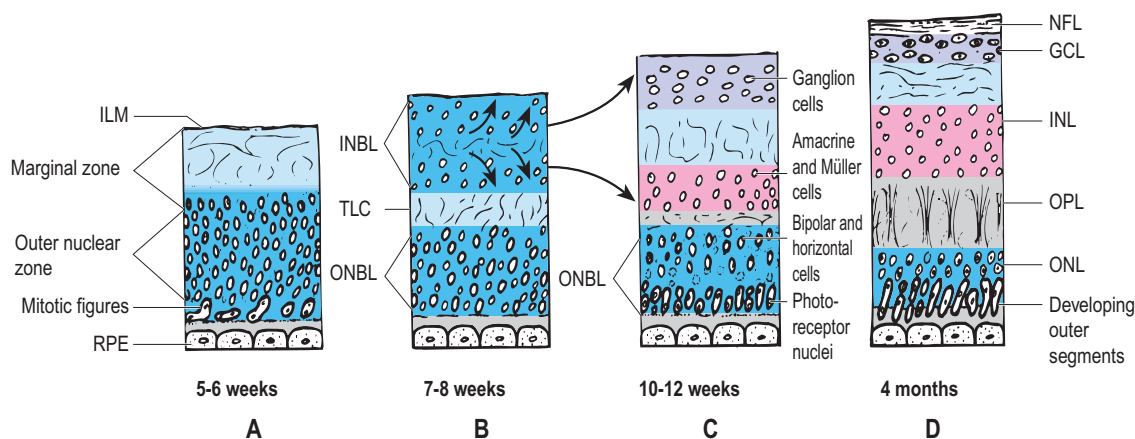


FIGURE 2-8 (A–D) Summary of early retinal morphogenesis in the human eye. Arrows indicate major patterns of cell movements. ILM, inner limiting membrane; RPE, retinal pigment epithelium; INBL, inner neuroblastic layer; ONBL, outer neuroblastic layer; TLC, transient layer of Chievitz; NFL, nerve fibre layer; GCL; ganglion cell layer; INL, inner nuclear layer; OPL, outer plexiform layer; ONL; outer nuclear layer.

inner plexiform layer) becomes identifiable at approximately 10.5 weeks of gestation, thereby obliterating the transient layer of Chievitz (Figs 2-8C and 2-9A). A new intermediate nucleated layer, the *inner nuclear layer*, becomes identifiable in the posterior pole retina and already contains the amacrine and Müller cell bodies, and shortly afterwards the bipolar and horizontal cells differentiate from the outer neuroblastic layer and migrate into this new nucleated layer (Fig. 2-8C). The remaining components of the outer neuroblastic layer will form the *outer nuclear layer* containing the cell bodies of the photoreceptors (rods and cones). The zone where fibres from this layer intermingle with those of the inner nuclear layer constitutes the new *outer plexiform layer* (Fig. 2-8D). The *external limiting membrane* (not a membrane *per se*) of the retina is identifiable in the earliest stages as rows of tight junctions between adjacent neuroblasts (Fig. 2-10B).

Further important landmarks in retinal development include:

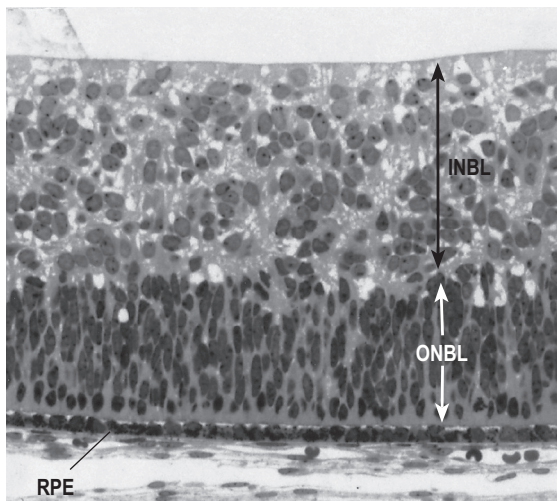
- synaptogenesis in cone pedicles at approximately 4 months, but not in rod spherules until 5 months
- photoreceptor outer segment formation commences around the fifth month
- horizontal cells become distinguishable around the fifth month

- microglia (resident tissue macrophages) invade the retina via the retinal vasculature and peripheral subretinal space (10–12 weeks onwards)
- the terminal expansions of the Müller cells beneath the inner limiting membrane mature around 4.5 months, at around the same time as their processes can be identified between the rods and cones.

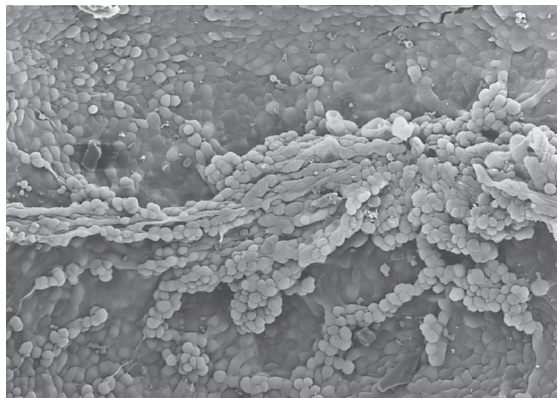
The onset of cellular differentiation in the neural retina is partly dependent on Shh (sonic hedgehog) and FGF signalling. In addition, a number of bHLH (basic helix-loop-helix, transcriptional activators) genes are likely involved in determining neuronal fate. NOTCH1 signalling appears to be involved in regulating the fate of the glial cells, particularly Müller cells.

MACULA AND FOVEAL DEVELOPMENT

Maculogenesis is first evident as a localized increase in ganglion cell density temporal to the optic disk at around 4.5 months. By 6 months, the ganglion cell layer may be eight or nine cells deep in this region. The thickened immature outer nuclear layer consists predominantly of immature cones. In the seventh month, there is a displacement of ganglion cells and formation of a *foveal depression*. There are approximately two layers of ganglion cells in the foveal region in the eighth month and at birth this is reduced to one. By 4 months postpartum the inner nuclear and

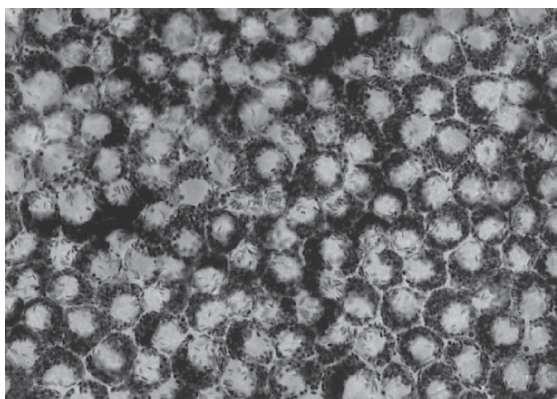


A

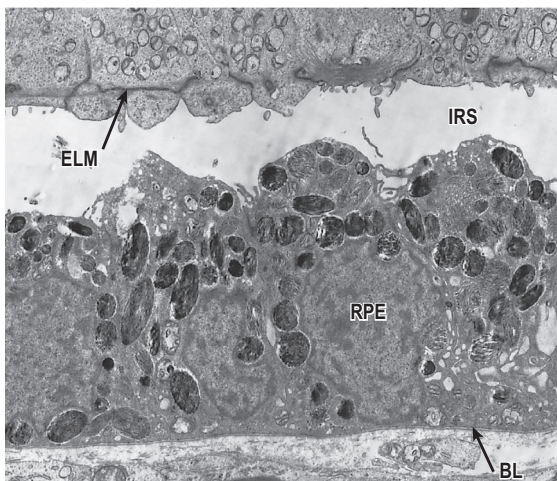


B

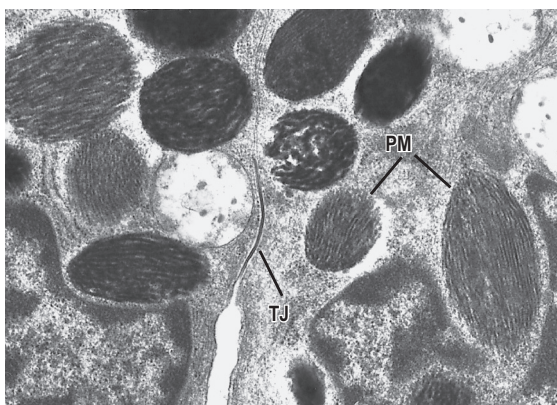
FIGURE 2-9 (A) Human fetal retina (12–13 weeks) showing inner and outer neuroblastic layers (INBL, ONBL). The inner neuroblastic layer has commenced differentiation and the transient layer of Chievitz is obliterated. RPE, retinal pigment epithelium. (B) Scanning electron micrograph of 'cords' of endothelial and supporting cells (retinal vessel precursors) ramifying on the retinal surface. Original magnifications: **A**, $\times 115$; **B**, $\times 55$.



A



B



C

FIGURE 2-10 (A) Human fetal RPE (15 weeks) viewed *en face* to demonstrate the regular hexagonal arrangement. (B) Transmission electron micrograph of human fetal RPE (12 weeks). ELM, external limiting membrane; IRS, intraretinal or subretinal space; BL, basal lamina. (C) Premelanosomes (PM) and tight junctions (TJ) near apices of human fetal RPE (22 weeks). Original magnifications: **A**, $\times 100$; **B**, $\times 4100$; **C**, $\times 16\,000$.

ganglion cell layers have receded to the margins of the fovea, leaving only cone nuclei in the foveal region. Elongation of the inner and outer segments occurs over the next few months.

PERIPHERAL RETINA

Until approximately 10–12 weeks of gestation the periphery of the retina extends to within 50–100 µm of the optic cup margin (Fig. 2-2F). By 14 weeks the retina terminates immediately posterior to the newly formed ciliary folds, with minimal pars plana. However, a definite pars plana and a poorly formed ora serrata are present by 6 months. The pars plana and the region from the ora serrata to the equator of the eye continue to grow after birth with continued growth of the eyeball, which occurs up to 2 years of age. The area of the retina is approximately 600 mm² at birth and reaches 800 mm² by 2 years.

DEVELOPMENT OF RETINAL VASCULATURE

The vessel incorporated into the choroidal fissure is the *hyaloid artery*, a branch of the ophthalmic artery, itself a branch of the internal carotid artery (Fig. 2-11A). The hyaloid artery, upon emerging from the centre of the optic stalk, spreads between the lens surface and the marginal zone of the primitive neural retina (lentoretinal space). With growth of the optic cup and formation of the vitreous cavity, the hyaloid artery elongates and courses through the primitive vitreous, within the *hyaloid canal*, to reach the posterior lens surface.

Early in the fourth month of development, temporal clusters, or angiogenic buds, develop from the hyaloid vessels at the optic disk. These strands consist of endothelial cells, future glial cells and macrophages (Fig. 2-9B). The endothelial cells are canalized and form new vessels that course along the nerve fibre layer towards the peripheral retina at approximately 0.1 mm per day, to reach the ora serrata by the eighth month. At the same time, dividing vascular endothelial cells penetrate the depth of the neural retina to the outer border of the outer nuclear layer, a process not completed until the ninth month. Here they form a polygonal network of vessels, the outer retinal plexus.

The intraneuronal portion of the hyaloid vessels becomes the *central retinal artery*. Developing

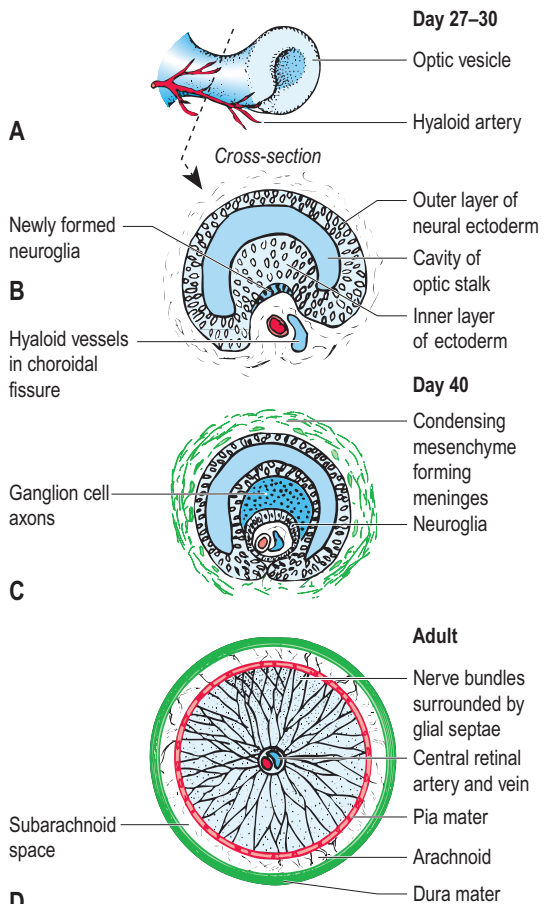


FIGURE 2-11 Diagram summarizing the major events in the development of the optic stalk and optic nerve.

capillaries are united by immature punctate tight and gap junctions and their basal laminae are incomplete.

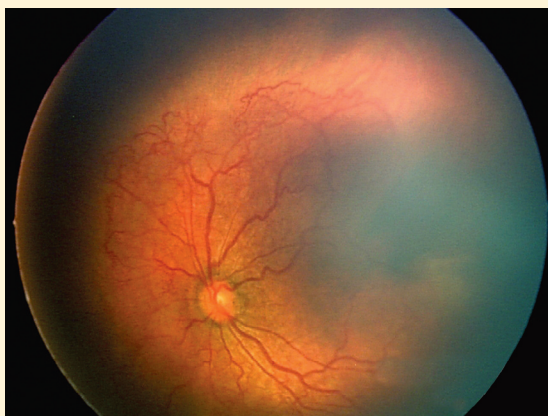
DEVELOPMENT OF THE RETINAL PIGMENT EPITHELIUM

One of the most dramatic events in eye development is the appearance of melanin in the embryonic RPE, which occurs as early as 28 days after fertilization (6–7 mm embryo). The RPE arises from the proximal cells of the optic vesicle which go on to form the outer layer of the optic cup (Fig. 2-1B,C). The presumptive RPE expresses the bHLH transcription factor *Mitf* (Fig. 2-4) and this appears to be dependent on canonical WNT signalling as evidenced in mice where inactivation of this signalling pathway causes the RPE to revert

BOX 2-3 CLINICAL CORRELATES

Retinopathy of prematurity

Altered oxygen tension has complex effects on the formation of capillary networks in the retina. Placing premature infants in high oxygen environments (to aid in their respiration due to the immature state of their lungs) can result in a delay or reduction in retinal vascularization. Upon returning to normal oxygen tension, the retinal tissues experience a relative hypoxia which induces the release of angiogenic factors (VEGF), resulting in episodes of abnormal neovascularization within the retina and vitreous, known clinically as *retinopathy of prematurity* (ROP) or *retrolental fibroplasia*. Progress in modern neonatal care in many countries has made possible the survival of premature infants born at gestational ages and birth weights that were once considered to offer little hope of viability. The incidence of ROP increases in prematurity as both a function of reduced birth weight and lower gestational age from approximately 40% in infants with birth weights 1101–1200 g to more than 90% in those with birth weights 501–600 g (image courtesy of Dr S. Tahija.)



to neural retina. Initially the RPE comprises a mitotically active pseudostratified columnar ciliated epithelium (Fig. 2-2B,C). The cilia disappear as melanogenesis commences. The RPE cells become hexagonal in shape and homogeneous in size (Fig. 2-10A) and in section appear as simple cuboidal epithelium (Fig. 2-10B), although a columnar morphology is maintained in the peripheral retina for a longer period. By the fourth month the RPE has only minimal apical microvilli, few or no basal infoldings, primitive basolateral interdigitations (Fig. 2-10B), mature apical junction complexes and intracytoplasmic premelanosomes (Fig. 2-10C).

Mitotic activity appears to take place early in development and is reputed to have ceased by birth; therefore, growth of the eye, and consequently of the RPE itself, is accommodated by hypertrophy or enlargement of the existing cells. A component of the future five-layered Bruch's membrane, the RPE basal lamina, is recognizable at the optic cup stage. Collagen fibrils are subsequently laid down beneath the basal lamina around 10 weeks; the first evidence of the elastic fibre layer can be detected around 3.5 months and by mid-term the elastic layer forms a fenestrated sheet.

Optic nerve and disk development

The hollow optic stalk forms a connection between the cavity of the forebrain (future third ventricle of the brain) and the cavity of the developing optic vesicles (Figs 2-1B and 2-2A). It is formed by the constriction of the proximal portion of the vesicle, particularly on the dorsal aspect concurrent with the expansion of the distal part (Fig. 2-11A). At this stage of morphogenesis (26–28 days) the central hollow fluid-filled stalk is lined by neuroectodermal cells. Invagination of the optic stalk at the 'choroidal' fissure, on the ventral aspect, which occurs simultaneously with invagination of the optic vesicle, results in a double layer of neuroectoderm with narrowing and eventual obliteration of the intervening fluid-filled cavity (Fig. 2-11B). The invagination process in the distal and ventral portions of the stalk leads to the incorporation of the hyaloid vessels and surrounding mesenchyme (Fig. 2-11B). The lips of the optic stalk start closing over the hyaloid vessels near the forebrain (5–6 weeks) and gradually extend distally. This fusion lags behind that of the cup. The optic stalks lie at approximately 65° to the mid-sagittal plane, compared with 40° in the adult.

Axons from developing retinal ganglion cells grow towards the optic stalk and, upon reaching the optic disk, change direction and course towards the brain among the inner neuroectodermal cells of the developing optic nerve. The choroidal fissure closes soon after, and by 6 weeks the optic nerve contains numerous axons that surround the hyaloid artery and vein. The outer neuroectodermal layer of the stalk differentiates into the peripheral glial mantle and the glial component of the lamina cribrosa. A cone-like structure,

BOX 2-4 CLINICAL CORRELATES

Malformations of the optic nerve head

When there is a failure of closure of the posterior part of the optic fissure, the optic nerve head is deformed by a *coloboma*, located inferonasally and associated with bulging of the sclera (scleractasia). The coloboma may take the form of a small recess (*optic pit*) at the rim of the disk where herniation of the retina occurs into the meninges and adjacent optic nerve. The clinical importance of an optic pit lies in its association with visual loss as a result of leakage from the pit and exudation of fluid beneath the macula.

AXIAL COLOBOMA OR ‘MORNING GLORY SYNDROME’

There are numerous names for a symmetrically enlarged and excavated optic disk – a condition that may be unilateral or bilateral. The most extreme axial malformation is the ‘morning glory syndrome’, so called because of the similarity to the American flower of the same name. This malformation is complicated by severe visual dysfunction and characterized by retrodisplacement of the optic disk into the meninges of the optic nerve. The abnormality is the result of a defect in mesodermal organization in the disk; the lamina cribrosa is not formed and there is fat and smooth muscle in the meninges.

Bergmeister’s papilla, consisting of glial cells and the remnants of hyaloid vessels, may persist at the optic nerve head in some individuals. An outer layer of condensed mesenchyme forms the optic nerve dura, which blends with the sclera. The glial septae surrounding the nerve bundles are composed of astroglia that differentiate from the cells of the inner layer of the optic stalk. The latter also gives origin to the oligodendroglia that surround the individual axons and are myelinated as far as the posterior margin of the lamina cribrosa. The nerve is displaced nasally during the third month by enlargement of the temporal side of the eye.

Development of the fibrous coat of the eye

Around weeks 6 and 7, periocular mesenchyme, derived from the neural crest and mesoderm (Fig. 2-5), begins to condense around the optic cup (Figs 2-1D,E and 2-2C,D). This mesenchyme can be differentiated into an *inner vascular layer* (uveocapillary lamina), which forms the stroma of the choroid, ciliary body and iris, and an *outer fibrous layer*, which will form the sclera and cornea.

DEVELOPMENT OF THE SCLERA

Mesenchymal condensation is most conspicuous at the future site of insertions of the extraocular muscles (limbal-equatorial region) (Fig. 2-2D). In the third month, active fibroblasts are already embedded in an irregular matrix of collagen, elastic fibrils and glycosaminoglycans. By 12 weeks a well-formed fibrous coat envelops the eye posteriorly as far as the optic nerve where the connective tissue forms a perforated plate, the lamina cribrosa, through which glia-covered ganglion cell axons pass.

DEVELOPMENT OF THE CORNEA

The surface ectoderm that seals over the lens pit forms the future corneal epithelium. It is a stratified squamous epithelium of three or four layers, the basal layer of which rests on a thin basal lamina. The first ‘wave’ of mesenchymal cells that passes over the optic cup margin migrates centripetally in the space between the anterior surface of the lens and the surface ectoderm to form the *corneal endothelium* (around 33 days) (Fig. 2-2C). Around day 49 a second ‘wave’ of mesenchyme commences migration from the optic cup margin and penetrates the space between the basal surface of the corneal epithelium and endothelium to form the *corneal stroma* (Fig. 2-2D). Both waves of mesenchyme are derived from the neural crest. The epithelium, which is continuous with the surface ectoderm, becomes stratified (three or four layers) and over the next few weeks the eyelids form and fuse (week 9–10) (Fig. 2-2D). Around 8 weeks the first evidence of loosely arranged collagen fibres can be detected amidst the actively synthetic fibroblasts, now known as *keratoblasts*. Within the corneal epithelium an intermediate layer of wing cells does not appear until the fourth or fifth month (Fig. 2-12A). The endothelium, which until now has been a double layer, becomes initially a simple cuboidal and ultimately a simple squamous layer resting on a thick basal lamina – the precursor of *Desemet’s membrane* (Fig. 2-12B). By this time all the corneal layers are present with the exception of *Bowman’s membrane*, which becomes identifiable by 5 months as an acellular collagenous zone beneath the epithelium (Fig. 2-12A). The stromal collagen bundles become organized into highly oriented *lamellae*, and the keratoblasts mature into long flattened *kerocytes*. This maturation process commences first in the

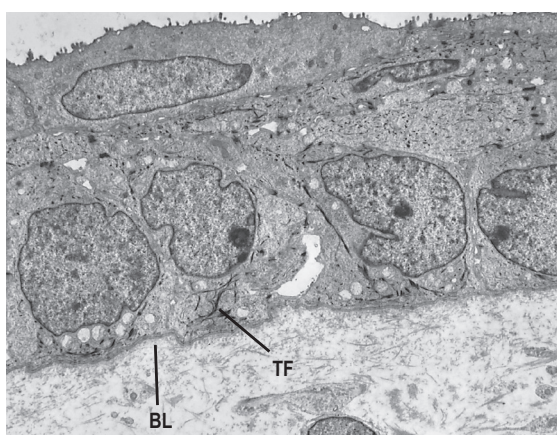
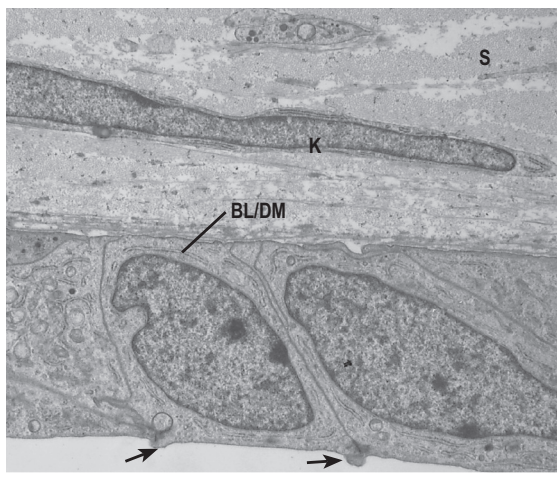
**A****B**

FIGURE 2-12 Transmission electron micrographs of human fetal cornea (16 weeks). **(A)** Epithelium consists of three cell layers joined by desmosomes resting upon a thin basal lamina (BL). Note the electron-dense intracytoplasmic tonofilaments (TF). **(B)** Developing endothelial cells. Note that the cells are cuboidal with apical junctional complexes (arrows) and rest on the basal lamina (BL/DM), which is already showing evidence of thickening to form the future Deszemet's membrane. K, keratoblast; S, collagenous stroma. Original magnifications: **A**, $\times 2300$; **B**, $\times 5000$.

posterior or deeper layers of the cornea and progresses more anteriorly or superficially.

Corneal thickness and diameter continue to increase throughout development by both interstitial growth (thickening of lamellae) and appositional growth (addition of new lamellae). The glycosaminoglycan constituents are known to alter during develop-

ment and are thought to underlie the initial swelling of the cornea (when lids are fused) and its subsequent thinning, which occurs during eyelid opening (24 weeks). Corneal transparency is gradually attained before birth owing to maturation of the superficial lamellae and the hydration activity of the endothelial cells. Innervation of the cornea commences at 3 months and reaches the epithelium at 5 months.

In summary, the cornea develops from the interaction of a surface ectoderm-derived epithelium and neural crest-derived mesenchyme, which gives rise to the deeper layers including Bowman's layer, stroma, endothelium and its thick basal lamina, Deszemet's membrane.

Development of the intraocular contents

LENS DEVELOPMENT (Fig. 2-13)

The thickened disk of ectodermal cells that forms the lens placode can be identified at 27 days. Differential elongation of these cells and contraction of their apical terminal bar causes the placode to invaginate, producing a lens vesicle with a central depression, the lens pit, leading into a hollow lens cavity that is connected briefly to the amniotic cavity via the lens pore (Figs 2-1C and 2-2B). As the vesicle, surrounded by its basal

BOX 2-5 CLINICAL CORRELATE

Corneal malformation (corneal leucoma)

Corneal opacification may be the result of a failure of the keratocytes to produce collagen fibres arranged in a lamellar array: instead, the pattern resembles sclera (scleralization of the cornea). *Peter's anomaly* is a term used to describe a posterior axial stromal defect associated with incarceration of the pupillary part of the iris at the edge of the defect. A mild form of malformation is the presence of thickening at the periphery of Deszemet's membrane (Schwalbe's line). When this is visible clinically (by gonioscopy) it takes the form of a bow: hence the term *embryotoxon* (Gk. *toxon* – a bow). Broad strands of tissue derived from the iris are sometimes seen in the chamber angle. In *Axenfeld's anomaly*, iridocorneal strands are localized to Schwalbe's line. When 'iris hypoplasia' is present, the malformation is known as *Rieger's* (or *Axenfeld–Rieger's*) anomaly (see Table 2-1 for gene mutations associated with these abnormalities).

lamina, detaches from the surface ectoderm (10 mm, 33 days) it sinks into the underlying rim of the optic cup (Figs 2-1D and 2-2B). Occasionally, degenerating cells (epithelial or periderm cells) are seen within the lens cavity (Fig 2-3). It now appears that lens induction is a multi-stage process requiring signalling by bone morphogenetic protein (Bmp) and also probably fibroblast growth factor (FGF) combined with the expression of a number of transcription factors, the most important of which appears to be *Pax-6*. More recently it has been shown that a disk-shaped 'pad' of modified extracellular matrix, consisting of fibronectin, produced by the lens placode, is critical to ensuring that the thickening of the surface ectoderm, destined to become the lens placode, is restricted to the area in close apposition to the optic vesicle and that disruption of this matrix leads to lateral spreading of the placode and failure to develop a lens placode – the so-called 'restricted expansion hypothesis'. These alterations in the surface ectoderm are *Pax-6* dependent as demonstrated by conditional knockout mice experiments.

The posterior cells of the lens vesicle elongate to form the *primary lens fibres* (Fig. 2-13A) and commence synthesis of a new group of intracytoplasmic proteins known as *crystallins*. Fibroblast growth factor, as well as being an inductive signal, is likely to be involved in lens fibre differentiation. The base of each elongating lens cell remains anchored to the basal lamina posteriorly and their apices grow towards the *anterior lens epithelium*, thereby obliterating the lens cavity (Figs 2-1D,E, 2-2C and 2-13B,C). The nuclei migrate forward within the elongated cell body to produce a *lens bow*, a row of cell nuclei with a conspicuous forward convexity (Figs 2-2F and 2-13C,H). Subsequent lens fibres arise from mitotic activity within the *anterior lens epithelium* at the equatorial zone and are known as *secondary lens fibres* (Fig. 2-13D,H). The tips of the secondary fibres extend around the primary fibres and meet at the Y-shaped anterior and posterior *lens sutures* (Fig. 2-13D). Every subsequent generation of fibres throughout embryonic, and indeed later, life is added superficial to the previous layer. Early in embryonic development the lens is nearly spherical or possibly longer in its antero-posterior axis; however, as secondary fibres are added at the equator the lens becomes more ellipsoid, a trend that continues until

BOX 2-6 CLINICAL CORRELATE

Malformations of the lens

The lens is particularly susceptible, during its formation and early growth, to intrauterine toxic insults such as rubella (German measles). The disorganization that ensues causes degeneration in the fibres and visible opacities in the lens (congenital cataract). If the lens fibre cells recover, the opacities become buried in the inner part of the cortex by the newly formed lens fibres.

Small (microphakic) or round (spherophakic) lenses do not exhibit a strikingly abnormal histology. Axial bulges on the anterior and posterior surfaces of the lens (anterior and posterior lentiglobus) are presumed to be the result of abnormalities in the lens epithelium and the lens capsule.

birth and then into adulthood. Basal lamina material is continually deposited by the lens epithelium on its external aspect and encases the lens in a membranous non-cellular envelope, the *lens capsule*. During embryonic and fetal development the lens receives nourishment via an intricate vascular net, the *tunica vasculosa lenti* (Fig. 2-13E–G), which completely encompasses the lens by approximately 9 weeks.

DEVELOPMENT OF THE VITREOUS AND HYALOID SYSTEM

At 5 weeks of gestation the lentoretinal space is narrow and occupied by the *primary vitreous* (Figs 2-1C,D, and 2-14A), which consists of the *hyaloid artery* and its branches, the *vasa hyaloidea propria*, which become incorporated into the optic cup through the choroidal fissure (Fig. 2-13G).

The *tunica vasculosa lenti* has two sources. The first (visible at around 5 weeks) is a series of capillaries that arise from the hyaloid vessels and form a palisade-like network of vessels, the *capsulopupillary vessels*, around the equator of the lens (Figs 2-13F and 2-14B). This capillary network anastomoses with the anterior component of the tunica, the *pupillary membrane* (*lamina iridopupillaris*), on the anterior lens surface (Fig. 2-14B). The pupillary membrane vessels are derived predominantly from branches of the long posterior ciliary arteries, which form an annular vessel close to the optic cup margin and whose branches pass over the rim of the optic cup to supply the anterior portion of the lens (Fig. 2-14B). The hyaloid system has no veins and venous drainage occurs anteriorly via the

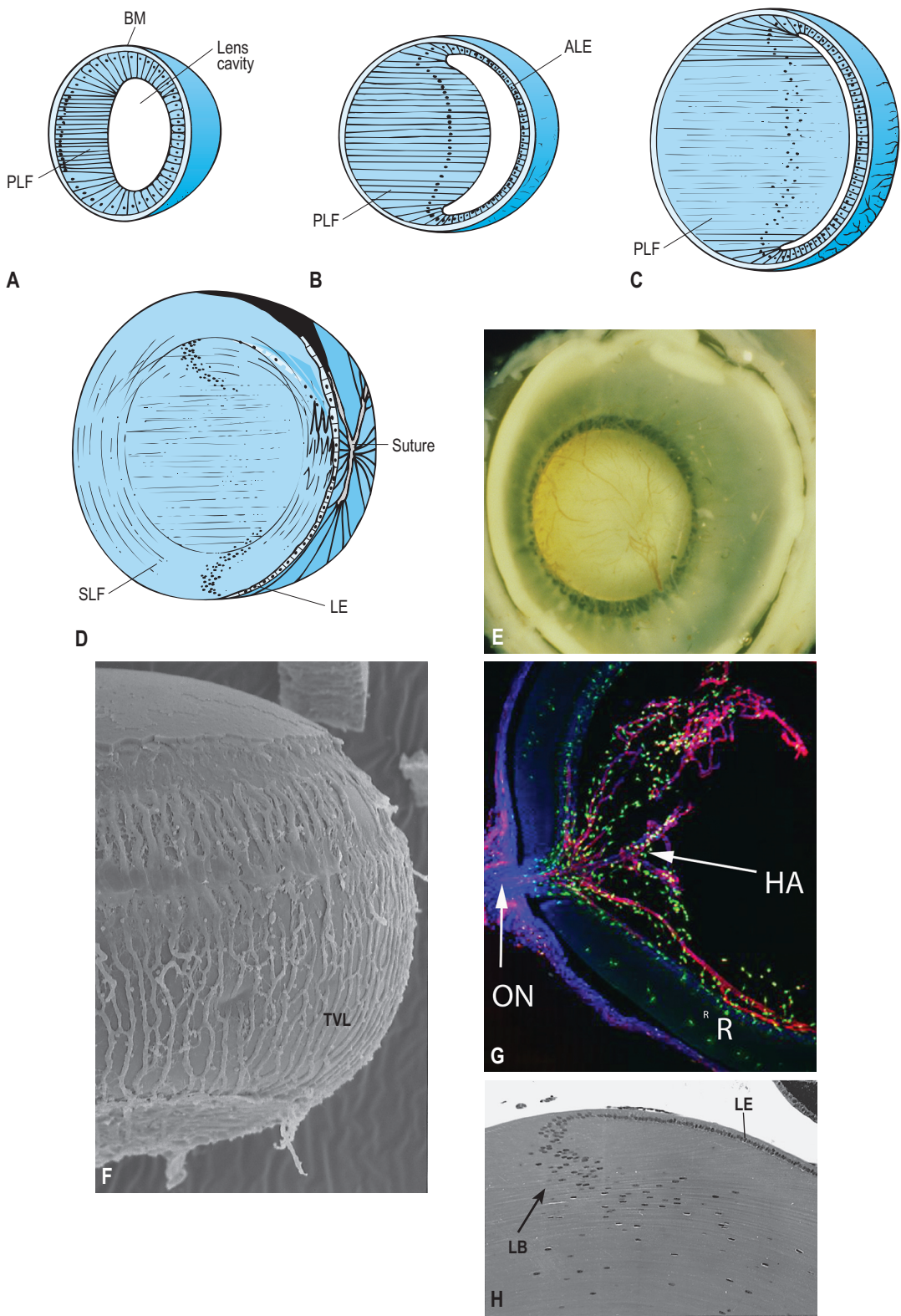


FIGURE 2-13

For legend see opposite page.

FIGURE 2-13 (A–D) Diagrammatic summary of lens morphogenesis. BM, basement membrane of lens cells; ALE, anterior lens epithelium; PLF, primary lens fibres; SLF, secondary lens fibres; LE, lens epithelium (former anterior lens epithelium). **(E)** Macroscopic view of human fetal eye (20 weeks) with posterior segment removed to reveal the hyaloid artery (HA) and tunica vasculosa lentis (TVL) around the lens. Original magnification: $\times 10$. **(F)** Scanning electron micrographic view of a fetal rat lens surrounded by the fine vessels of the TVL. Note the small spherical macrophages associated with the vessels on the lens surface. Original magnification: $\times 95$. **(G)** Frozen section of P0 mouse eye (day of birth) showing hyaloid artery emerging from the optic nerve and ramifying in the vitreous. The lens has been removed. The mouse is a Cx₃cr1-GFP transgenic mouse in which all myeloid-derived cells (monocytes, macrophages, microglia) are fluorescent green. Vessels are stained red and blue represents nuclei: $\times 30$ (Courtesy of Dr Wai Wong). **(H)** Fetal lens showing the lens bow (LB) arising from the equatorial region. LE, lens epithelium. Original magnification: $\times 90$.

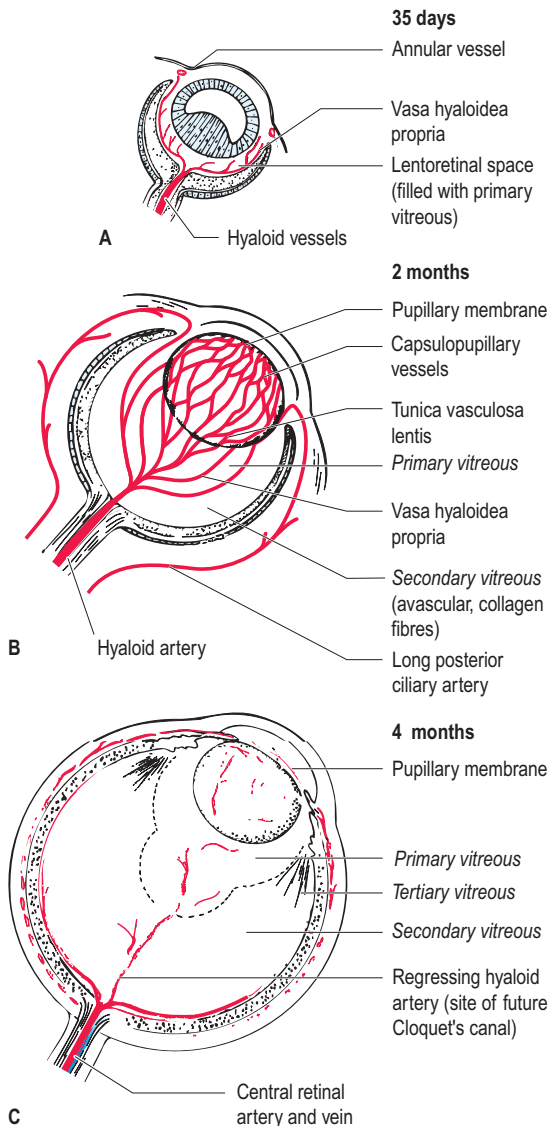


FIGURE 2-14 Early development of the vitreous and hyaloid system.

pupillary membrane and the uveal vessels. The expression of vascular endothelial growth factor by the lens is thought to be a critical molecular event in the formation of the hyaloid vascular system.

An avascular *secondary (definitive)* vitreous composed of finely fibrillar material is deposited behind the primary vitreous between 5.5 and 12 weeks. The primitive hyalocytes, widely recognized as belonging to the mononuclear phagocyte system, arise at this time and likely derive from the same population as the macrophages associated with the hyaloid artery and tunica vasculosa lentis (Fig. 2-13G). These cells also give rise to the microglia of the retina and are all derived in embryonic life from yolk sac precursors – namely the origin of haematopoietic cells prior to this role being assumed by the liver and later the bone marrow. Mesenchymal cells in the adventitia of vitreal vessels likely contribute to the vitreous matrix. Much of the hyaluronan and collagen (type II) in the vitreous gel is added after birth.

Around the end of the third month distinct condensations of secondary vitreous become evident in the space between the optic cup margin and the lens. The fibres, which are firmly attached to the inner limiting membrane of the retina in the developing pars plana region, are sometimes referred to as the *tertiary vitreous* and, when mature, will form the *vitreous base* (Fig. 2-14C). It seems likely that the non-pigmented ciliary epithelial cells in this region are responsible for synthesis of the tertiary vitreous and zonular fibres.

During the fourth month the remains of the primary vitreous, the hyaloid vessels and the vasa hyaloidea propria, together with the tunica vasculosa lentis, begin to atrophy (Fig. 2-14C). The regression occurs contemporaneously with the formation of the retinal vasculature. The remnant of the course these vessels

took through the vitreous is evident in the adult as a narrow fluid-filled central channel, Cloquet's canal. Macrophages play an important scavenging role in the regression of the hyaloid vessels (Fig. 2-13E,G) and may also be responsible for the induction of apoptosis of vascular endothelial cells. Small portions of the pupillary membrane may persist in otherwise normal newborn eyes.

BOX 2-7 CLINICAL CORRELATES

Malformations of the vitreous and hyaloid artery system

Normally, the hyaloid system of vessels vanishes completely but in some disorders regression does not occur.

PERSISTENT TUNICA VASCULOSA LENTIS

Persistence of the anterior part of the tunica vasculosa lenti or the pupillary membrane causes deformation of the iris.

PERSISTENT HYPERPLASTIC (ANTERIOR) PRIMARY VITREOUS

If the embryonic fibrovascular tissue in the anterior vitreous face persists, the ciliary processes are drawn internally, providing a valuable clinical diagnostic feature that is visible when the pupil is dilated. The lens is opaque in persistent hyperplastic anterior primary vitreous, because a retrolental fibrovascular mass erodes the posterior lens capsule and penetrates the lens cortex. The white retrolentinal mass (leucocoria) produced by this malformation can lead to a mistaken clinical diagnosis of retinoblastoma.

PERSISTENT (POSTERIOR) HYPERPLASTIC PRIMARY VITREOUS

A persistent hyaloid artery and the condensed posterior primary vitreous project from the optic disk and the adjacent retina. Distortion of the disk by prepapillary and preretinal fibrous membranes is associated with radial or falciform folds in the retina. Although many cases appear sporadic, there has been some evidence for mutations in *LRP5* and *FZD4* genes and also defects in apoptosis and WNT signalling indicating these processes may be critical to the normal regression of the hyaloid vascular system. In addition, mice lacking the Arf tumour suppressor protein (usually produced in response to sustained mitogenic activity and important in controlled apoptosis) fail to resorb the hyaloid system and this leads to persistence of pericyte-like cells that proliferate and destroy the lens and retina, causing blindness.

Development of the uveal tract

THE CHOROID

The choroid arises very early in development from the loose vascular layer of mesenchyme that surrounds the optic cup (Fig. 2-1C,D). A palisade layer of vessels lies immediately external to the RPE and forms the basis of the future choriocapillaris. Fenestrations in the endothelium become evident very early in development. This layer of vessels forms communications with the precursors of the posterior ciliary arteries at around 2 months. A second layer of vessels forms at around 4 months external to the future choriocapillaris and consists of thin-walled venous channels that will eventually unite to form rudimentary vortex veins and branches of the long and short posterior ciliary arteries. An intermediate or middle layer (future Sattler's layer) of mainly arterioles forms between the larger vessels (Haller's layer) and the choriocapillaris. The choroidal vessels are initially embedded in a loose collagenous stroma; however, elastic fibres form later in development in the outer choroid (future lamina suprachoroidea) and pigment-bearing melanocytes appear around the seventh to eighth month of gestation.

THE CILIARY BODY

The development of the ciliary body has similarities to iris development because it involves an interaction between mesenchyme and neuroectoderm. Ciliary body and iris development commence in the 11–12th week with indentation of the outer pigmented layer of the neuroectoderm (presumptive pigmented ciliary epithelium) near the optic cup rim by small capillaries in the inner vascular mesenchyme (Fig. 2-15A,B). Investigations of *Hox* gene expression during early ocular development in the mouse revealed a highly restricted expression of *Hox 7.1* in the non-pigmented or inner neural epithelium just behind the optic cup margin at the site of the prospective ciliary body and iris. This gene is expressed 2 days before any morphological evidence of these structures is evident and thus it may be an early molecular marker for regional specialization and differentiation in the eye.

Initially, the inner non-pigmented ciliary epithelium is flat, but as the vascular sprouts enlarge they push inwards to form primitive radial folds. This arrangement of a vascular connective tissue core

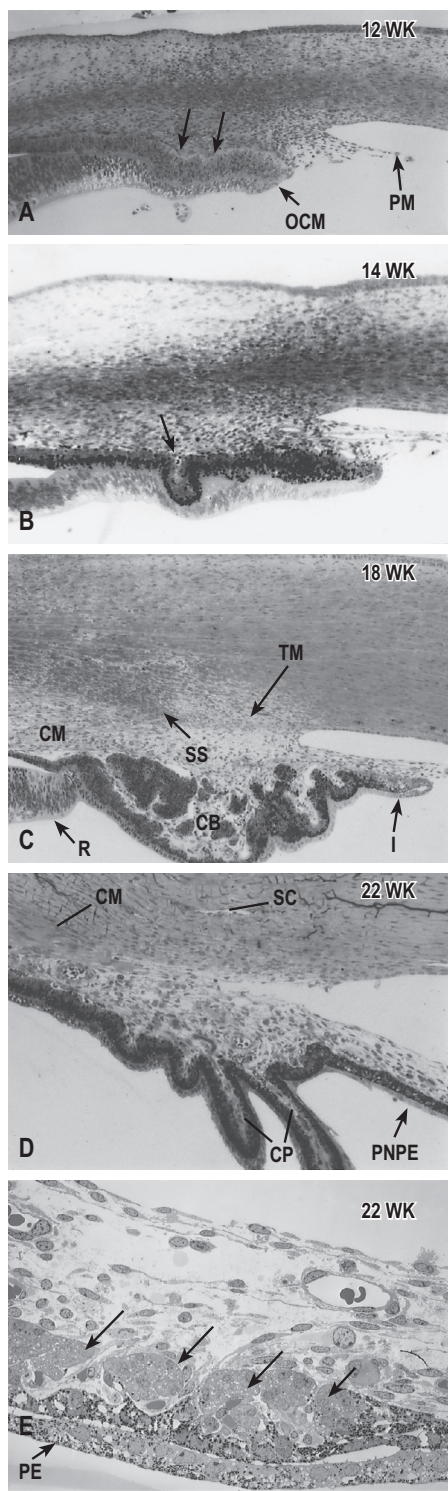


FIGURE 2-15 (A–D) Development of the ciliary body and iris in the human fetal eye from 12 to 22 weeks (the lens has been removed in all specimens). Note that the earliest evidence is the vascular mesenchyme indenting the outer neuroectoderm layer (arrows) near the optic cup margin (OCM) in 12- and 14-week specimens. PM, pupillary membrane; CM, ciliary muscle; SS, scleral spur; TM, trabecular meshwork anlage; I, iris; CB, ciliary body; R, retina; SC, Schlemm's canal; PNPE, posterior non-pigmented epithelium of the developing iris; CP, ciliary processes. **(E)** Electron micrograph of iris margin in a 22-week-old human fetal eye to illustrate sphincter pupillae smooth muscle bundles (arrows) differentiating from the anterior pigmented iris epithelium. Note that the posterior epithelium (PE) is showing early evidence of melanogenesis. Original magnifications: **A**, $\times 75$; **B**, $\times 95$; **C**, $\times 110$; **D**, $\times 80$; **E**, $\times 420$.

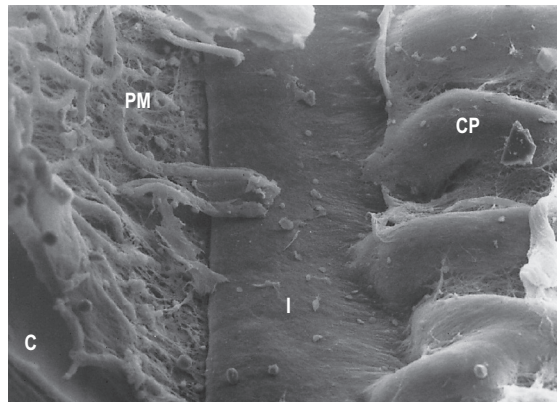


FIGURE 2-16 Scanning electron micrograph of the developing human ciliary processes and iris (20-week fetus). Note the smooth outline of the ciliary processes (CP), the short iris (I), and vessels of the pupillary membrane (PM). C, cornea. Original magnification: $\times 120$.

overlaid by a double layer of ciliary epithelial cells forms the basis of adult ciliary process anatomy (see Ch. 1). The 70–75 radial folds that develop in this manner appear initially as smooth undulations (Figs 2-15B and 2-16); however, between weeks 14 and 22 they increase in height and complexity (Fig. 2-15C,D). Early in development the primitive neural retina terminates immediately posterior to the ciliary folds (Fig. 2-15C), but later a smooth area, the future *pars plana*, separates the two regions and continues to expand during the remainder of gestation with continued growth of the eye. The ciliary epithelium may commence aqueous production as early as 20 weeks, coinciding with concomitant changes in the iridocorneal angle.

The ciliary muscle differentiates at around 15 weeks' gestation from the mesenchyme between the neuroectoderm and scleral condensation external to the early ciliary folds, namely the region that will form the future ciliary body stroma. The longitudinally oriented smooth muscle fibres terminate in the region of the trabecular anlage during fetal development. Circular or radial ciliary muscle fibres do not differentiate until much later in development and indeed are not fully formed until about 1 year of age.

THE IRIS

Until 12–13 weeks of development there are no morphological signs of iris differentiation at the rim of the optic cup, and the cup margin lies posterior to the lateral recess of the anterior chamber (Fig. 2-15A). At around 14 weeks there is an expansion or growth of neuroepithelial cells at the cup margin anterior to the presumptive ciliary body (Fig. 2-15B,C). The optic cup neuroectoderm grows in a centripetal manner between the mesenchyme that has formed the cornea and the anterior lens surface. As it grows it incorporates some of the vessels of the lamina iridopupillaris or pupillary membrane, which lie on the anterior surface of the lens. This vascular mesenchyme is effectively split by the centrally growing neuroepithelial cells into vessels of the iridopupillary membrane, which now face the anterior chamber and form the future iris stroma (Fig. 2-15C,D), and deep to the epithelium the vessels of the capsulopupillaris.

The smooth muscles of the iris, the *sphincter* and *dilator pupillae* muscles, are unique in embryological terms because they differentiate directly from neuroectoderm. The sphincter pupillae differentiation commences before that of the dilator pupillae. Around 13–14 weeks, anterior iris pigment epithelial cells delaminate, lose their melanin, develop intracytoplasmic microfilaments (actin) and dense bodies, and deposit a basal lamina. These are classic characteristics of smooth muscle cells. Cell-to-cell contact (gap junctions) among the smooth muscle cells in this circumferential muscle band is not fully established until 7 months (Fig. 2-15E), and the muscle becomes free in the stroma at around 8 months. The dilator pupillae muscle develops much later, around 6 months, as basal extensions of the anterior or pigmented

epithelial layer of the iris (Fig. 2-17), and continues to develop even after birth. These basal extensions are arranged radial to the pupil. This muscle never becomes fully independent of the epithelium because, even in adulthood, it is composed of modified basal processes of the neuroepithelial cells (Fig. 2-17).

During development the posterior (inner) iris epithelium is largely amelanotic. It is continuous with the non-pigmented ciliary epithelium and thus the neural retina. Intracytoplasmic melanin increases in the fourth month, initially near the pupil margin (Fig. 2-15E), and by months 7–8 this layer is heavily pigmented (Fig. 2-17) and the anterior layer has lost its pigment.

Iris innervation, both adrenergic and cholinergic, is not established until late in development. In common with the choroid, pigment-bearing melanocytes are not identifiable in the iris stroma until late in development, around birth or later (Fig. 2-17). The thickness of the stroma and degree of melanogenesis are determining factors in eye colour at birth, and indeed full pigmentation and the pattern of the anterior surface are not complete until a few years postpartum. Blue irides are the result of interference and reflection of light from stromal collagen, whereas a thin stroma

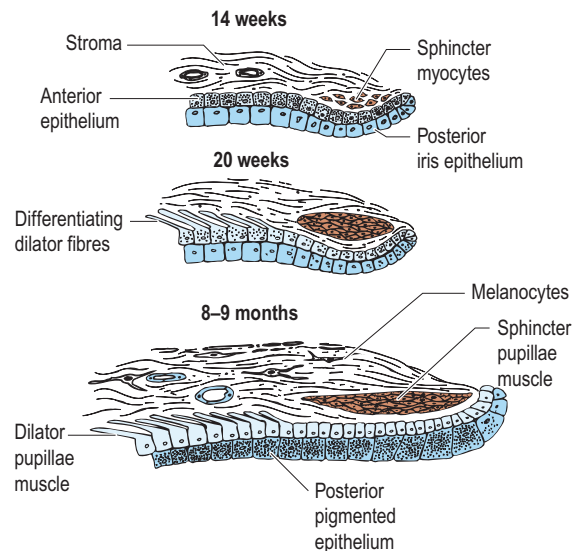


FIGURE 2-17 Summary of human iris development showing the differentiation of the sphincter and dilator pupillae from the anterior iris epithelium (neuroectoderm).

BOX 2-8 CLINICAL CORRELATES

Aniridia

Aniridia is a rare autosomal dominant bilateral disease in which there is an apparent absence of the iris. The term is a misnomer because histologically the abnormal iris is seen as a stump of hypercellular stroma, often with an abnormal proliferation of the pigment epithelium. Malformation or hypoplasia of the outflow system occurs in aniridia, as do anterior and posterior cortical lens opacities. The lens may dislocate (ectopia lentis) and the optic nerve may be hypoplastic. It is now well known that aniridia is caused by mutations of the *Pax-6* gene.

may allow the brownish colouration of the posterior epithelium to show through. Later in life, brown irides are the result of heavily pigmented melanocytes within the stroma.

Development of the anterior chamber angle and aqueous outflow pathways

As early as the 12th week a roughly wedged-shaped distinctive mass of mesenchyme, the trabecular anlage, can be identified at the junction of the pupillary membrane and lateral margins of the cornea, namely the future anterior chamber angle (Figs 2-15A and 2-18). The trabecular anlage consists of a dense collection of stellate mesenchymal cells (neural crest-derived) and some loosely arranged extracellular matrix (Fig. 2-18A,D). The deep aspect of the wedge-shaped anlage is characterized by a row of small capillaries (Fig. 2-18A), which most probably have grown in from the capillary plexus on the external surface of the eye (future episcleral plexus) and are thus lined by mesoderm-derived vascular endothelial cells. By weeks 20–22 (fifth month) the connective tissue matrix of the trabecular anlage consists of flattened ‘trabecular’ endothelial-lined sheets and cords (early trabeculae) separated by intervening spaces (Fig. 2-18). On the deep aspect of the fetal trabecular meshwork the collection of small capillaries fuses to form a single elongated slit-like vessel, the *canal of Schlemm*, lined by endothelial cells that are continuous with those of the collector channels and episcleral vessels. The characteristic ‘giant vacuoles’ (eFig. 2-3B)

BOX 2-9 CONGENITAL GLAUCOMA

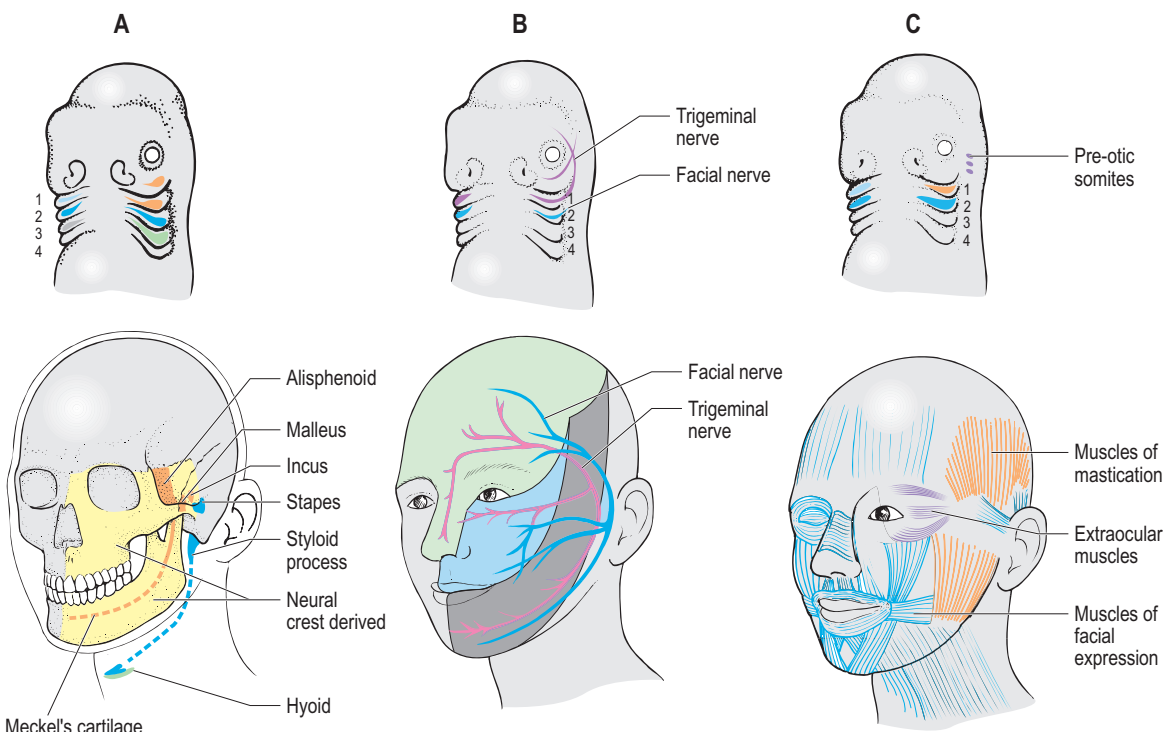
Whilst there have been many theories on the aetiology of congenital glaucoma it appears to be a failure of differentiation or alterations in differential growth rates. This is a strong candidate because the few pathological accounts of congenital glaucoma describe the tissue as undifferentiated, or as lacking the typical organized trabeculae and intertrabecular spaces, especially in the outer or cribriform zone. Mutations in *CYP1B1*, *LTP2* and *MYOC* have been found in a cohort of primary congenital glaucoma patients and the *CYP1B1* gene, which encodes cytochrome P450 1B1, a member of the cytochrome P450 superfamily of enzymes. It may metabolize a signalling molecule involved in eye development, possibly a steroid; hence, mutations may lead to congenital glaucoma.

CHAMBER ANGLE MALFORMATION (GONIODYSgenesis)

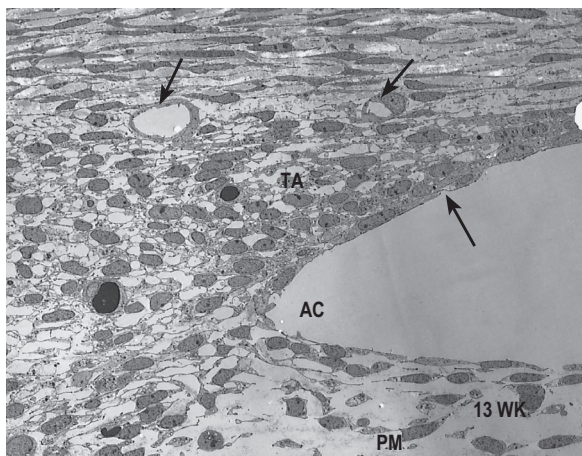
A failure of remodelling of the progenitor tissue in the angle leaves very obvious strands between the iris stroma and the trabecular meshwork, or between the iris and cornea. Abnormalities in the outflow system, ‘goniodysgenesis’, include hypoplasia of the scleral spur with extension of the ciliary muscle into the outer part of the trabecular meshwork and an excessive amount of trabecular tissue. In addition, there are a number of more generalized abnormalities of the mesenchyme and mesoderm, which display altered iridocorneal angle structure and may manifest as infantile glaucoma. These include posterior embryotoxon, Axenfeld syndrome, Rieger’s anomaly and Peters’ anomaly. A number of mutations or deletions have been associated with iridogoniodysgenesis (Table 2-1).

in the canal endothelium that are responsible for the passage of aqueous across the inner wall of the canal (see Ch. 1) appear at around 18–20 weeks of gestation.

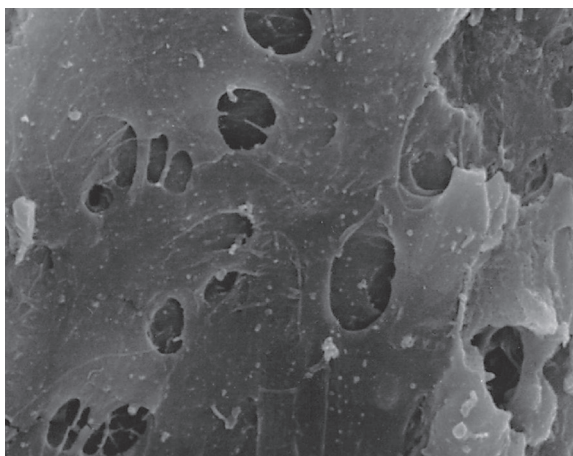
During the remainder of fetal development the meshwork becomes further specialized into cord-like inner uveal trabeculae, numerous intermediate layers of lamellar corneoscleral trabeculae, and a deep loosely arranged cribriform meshwork (Fig. 2-18B). The scleral spur is formed by month 4–5 (Fig. 2-15C). Scanning electron microscopy of the developing angle reveals that the inner aspect of the developing uveal meshwork is incomplete and numerous perforations allow communication between the anterior chamber and the spaces of the developing meshwork from 15 weeks onwards (Fig. 2-18C).



eFIGURE 2-3 Summary of the embryonic pharyngeal arches and their derivatives in the adult. (A) Arch cartilages (yellow shaded areas represent bones derived from the neural crest); (B) arch nerves and the sensory territories of the three divisions of the trigeminal nerve shaded green (V_1), blue (B_2) and grey (V_3) (see also Fig. 1-55); and (C) arch musculature.



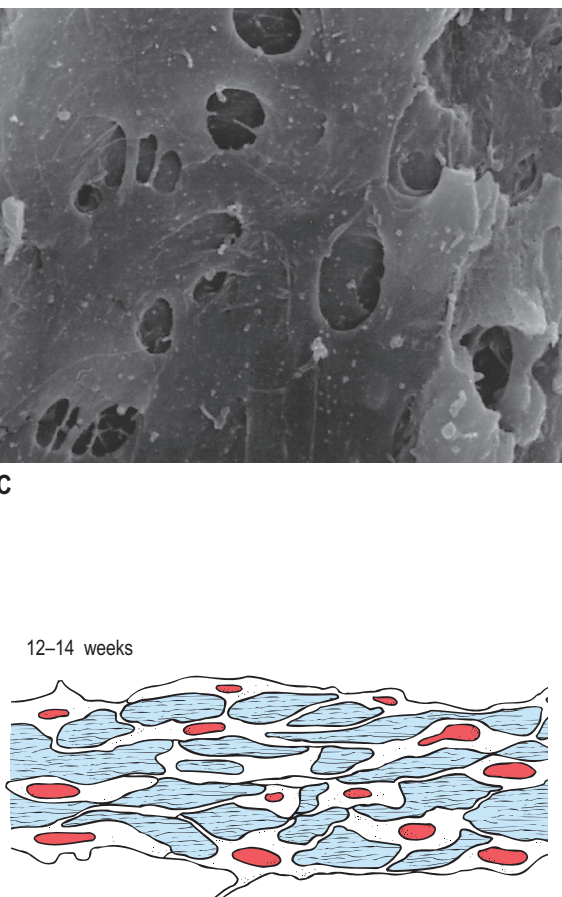
A



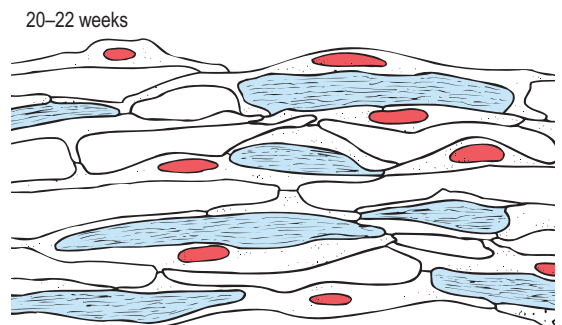
C



B



12–14 weeks



20–22 weeks

FIGURE 2-18 Development of the iridocorneal or chamber angle (see also Fig. 2-16). (A) Electron micrograph of the trabecular anlage (TA) in a 13-week-old human fetus. Note the two small capillaries (arrows) on the deep aspect of the anlage, the high density of trabecular cells, and the poorly developed extracellular matrix. AC, anterior chamber; PM, pupillary membrane (future iris stroma). Original magnification: $\times 500$. (B) Electron micrograph of the trabecular meshwork in a 22-week-old human fetus. Note the enlarged intratrabecular spaces separated by well-formed connective tissue trabeculae and the size of Schlemm's canal (SC), which possesses giant vacuoles (GV) in its inner wall. Original magnification: $\times 100$. (C) Scanning electron micrograph of the inner surface of the trabecular anlage in a 13-week-old human fetus revealing the incomplete nature of the endothelial cells facing the anterior chamber. These perforations most likely allow free passage of cells and fluids from the anterior chamber to the developing meshwork from this early stage onwards. Large arrow in (A) indicates the perspective from which the scanning micrograph was obtained. Original magnification: $\times 1600$. (D) Summary of the morphogenetic changes that occur during remodeling of the loose mesenchyme of the trabecular anlage to form the trabecular meshwork. (Parts A–C from McMenamin, 1989, 1991; with permission.)

Development of the extraocular muscles

The extraocular muscles are some of the few periocular tissues that have been shown not to be of neural crest origin (Fig. 2-6). They are thought to arise from presumptive myocytes in the *preotic region* (*paraxial mesoderm*) in the area of the prochordal plate (eFig. 2-3).

They migrate ventrally and caudally around the developing eye. The presumptive myocytes concentrate particularly in the equatorial zone external to the mesenchymal condensation, which forms the sclera. Here they proliferate and differentiate. Their flattened connective tissue tendons, which are of neural crest origin, eventually fuse with the sclera.

Investigations of *MyoD* gene expression in transgenic mice (using the *LacZ* reporter gene) have shown evidence of myogenesis *in situ* around the developing eye as early as E10.5 (day 10.5 of embryogenesis), at about the time when myocytes are appearing in the hyoid arch mesenchyme.

The extraocular muscles appear in approximately the following sequence: lateral rectus, superior rectus and levator palpebrae superioris (week 5), superior

oblique and medial rectus (week 6), followed by inferior oblique and inferior rectus (common primordium).

The axons of the *general somatic efferent neurones* of cranial nerves III, IV and VI, which innervate these muscles, are ‘dragged’ behind the migrating myocytes from the site of their cell bodies in the developing brainstem to the periocular region.

Development of the eyes and surrounding structures is influenced by the pattern of development of the skull, pharyngeal arches and face

A detailed account of the embryology of the head, skull and face pertinent to understanding the development of the eye and orbit can be found at <https://expertconsult.inkling.com/>. See also Video 1-2.



FURTHER READING

A full reading list is available online at <https://expertconsult.inkling.com/>.



DEVELOPMENT OF THE SKULL

The orbit lies at the junction of the neurocranium (skull vault) and viscerocranum (facial skeleton), and has also evolved partly from the primitive sensory capsules around the eyes. Therefore, to understand the embryology and development of the orbit, it is essential to appreciate that the entire craniofacial skeleton is formed by a combination of several components.

CHONDROCRANUM

The *chondrocranium* forms the skull base initially as cartilaginous precursors that develop in a rostral to caudal sequence, namely the prechordal plate, hypophyseal and parachordal cartilages. These subsequently ossify to form the midline bones in the base of the skull from the interorbital region (body of the sphenoid) to the occipital region. The sensory capsules that evolved to support the olfactory organs, eyes and inner ear develop separately alongside this midline basal cartilage. These capsules develop initially as cartilage and in humans are represented by bones in the nasal cavity (ethmoid from prechordal cartilages), orbits (body of the sphenoid – hypophyseal cartilages, lesser wing, and medial part of the greater wing of the sphenoid) and part of the temporal bone.

MEMBRANOUS BONES

The *membranous bones*, evolved from ‘dermal’ bones like those seen in fossils of primitive placoderm fishes, ossify directly from mesenchyme (‘in membrane’). They are derived from neural crest and parachordal (head) mesoderm and form the calvaria or cranial vault in the human skull. They are represented in the orbit by the orbital plate of the frontal bone.

Viscerocranum

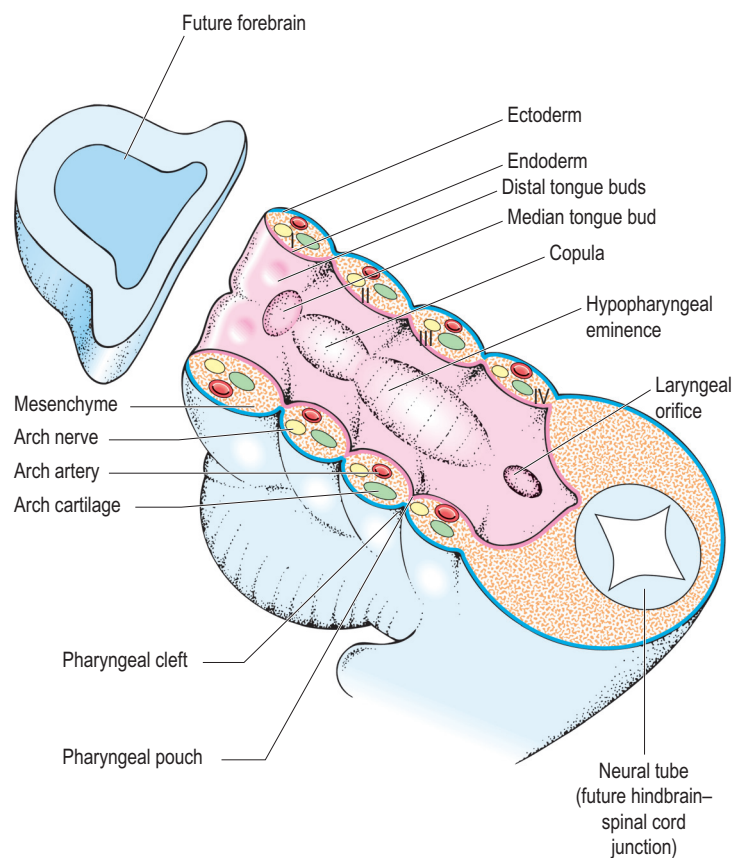
The *viscerocranum* evolved to support the *branchial (gill) arches* in fish. In humans there are five pairs of *pharyngeal arches*, either side of the foregut tube, whose derivatives contribute to the viscerocranum (see below).

The Pharyngeal Arches

The pharyngeal arches play an important role in the morphogenesis of the head and neck; the first and second

arches in particular are important to the development of the periocular region. Pharyngeal arches form in a craniocaudal sequence and are not all at similar stages of development at any point in time. In humans, five arches develop that correspond to arches 1, 2, 3, 4 and 6 of their evolutionary precursors in fish. The first or mandibular arch has two components, one forming the upper jaw the other the lower jaw; the second or hyoid arch has evolved to support the jaw, tongue and larynx (eFig. 2-3). The third arch also contributes to the hyoid. The fourth and sixth arches help form the larynx. Each arch has an inner covering of endoderm (separated by endodermal *pharyngeal pouches*) and an outer covering of ectoderm (separated by ectodermal *pharyngeal clefts*), a cartilaginous component (e.g. Meckel’s cartilage), an arch nerve and an arch artery, together with a core of mesenchyme (eFig. 2-4). This mesenchyme is a mixture of somatic mesoderm and neural crest-derived mesectoderm (derived from rhombomere 2 (first arch), rhombomere 4 (second arch) and rhombomere 6 (third arch); (Hunt et al., 1991; Noden, 1991; Maden et al., 1992; Hall, 2005)). eTable 2-1 and eFigure 2-3 summarize the skeletal, neuronal and muscular derivatives from the pharyngeal arches. The migration of neural crest cells into each of the pharyngeal arches is like all axial organization (i.e. neural tube, somitic mesoderm and endoderm) controlled by the *Hox* code. Only a few elements of the viscerocranum, such as the medial part of the greater wing of the sphenoid (alisphenoid), incus, malleus and stapes, arise directly from the cartilaginous component (eFig. 2-3A); the majority of the cartilaginous elements of the pharyngeal arches regress and become encased within membrane bones that ossify directly from neural crest-derived mesenchyme. Such membranous bones include the maxilla, zygoma, squamous temporal bone and dentary (described in most textbooks as the mandible) (eFig. 2-3A).

Some of the cranial nerve sensory neurones (part of V, VII, IX and X), like the dorsal root ganglia of the trunk, arise from the neural crest, as do the four parasympathetic ganglia of the head and neck.



eFIGURE 2-4 Schematic diagram of the floor of the embryonic mouth as viewed from above in a horizontal section of the head. Note the pharyngeal arches (I–IV) have been cut to expose their neural (yellow), arterial (red), cartilaginous (green) and mesenchymal (orange stipple) contents. The arches are lined externally by ectoderm (blue) and internally by endoderm (purple).

eTABLE 2-1 Pharyngeal arch derivatives (arch arteries and their derivatives not included)

| Pharyngeal arch | Pouch endoderm | Skeletal elements | Cranial nerve | Muscles | |
|-----------------|--|---|---|---|---|
| | | Ossify in cartilage | | Ossify in membrane | |
| 1 | Tympanic cavity Pharyngotympanic tube (cleft ectoderm – external auditory meatus) | Arch cartilage – palatoquadrate bar: alisphenoid, incus Meckel's cartilage – malleus | Arch mesenchyme: <i>upper part</i> – maxilla, zygoma, squamous temporal bone <i>lower part</i> – mandible | Maxillary division of trigeminal (V) (upper part of arch 1) Mandibular division of trigeminal (V) (lower part of arch 1) | <i>From cranial somitomere 4:</i> Muscles of mastication (temporalis, masseter, pterygoids) plus mylohyoid, anterior belly of digastric, tensor tympani, tensor veli, palatini |
| 2 | Epithelial lining of tonsillar crypts and tonsillar fossa | Reichert's cartilage: stapes, stylohyoid ligament, upper part of hyoid | Facial nerve (VII) | <i>From somitomere 6:</i> Muscles of facial expression plus posterior belly of digastric, stylohyoid, stapedius | |
| 3 | Dorsal wing – inferior parathyroid Ventral wing – epithelioid cells of thymus (Hassall's corpuscles and epithelial reticulum) | Lower part of hyoid | Glossopharyngeal nerve (IX) | <i>From somitomere 7:</i> Stylopharyngeus | |
| 4 | Dorsal wing – superior parathyroid Ventral wing – ultimobranchial body: C cells in thyroid gland | | Upper laryngeal cartilages (mesoderm) | Superior laryngeal branch of vagus nerve (X) | <i>From occipital somites 2–4:</i> Pharyngeal constrictors, cricothyroid, levator veli palatini |
| 6 | | | Lower laryngeal cartilages (mesoderm) | Recurrent laryngeal nerve (X) | Intrinsic muscles of the larynx |

The accessory nerve has all the hallmarks of a branchial arch nerve as its cell bodies in the brainstem and cervical spinal cord are in line with other branchial efferent cell bodies (branchial efferent column); however, its evolutionary history, or more specifically the muscles it supplies (sternocleidomastoid and trapezius), is controversial, as are many of the musculoskeletal elements of the neck and shoulder (Matsuoka et al., 2005).

DEVELOPMENT OF THE FACE

(eFig. 2-5)

Development of the face commences around the fourth week and is largely complete by week 10. The basic arrangement of the face is the result of fusion of five swellings around the stomodeum (primitive mouth), nasal pits and eyes. There are paired maxillary and mandibular processes plus an unpaired fronto-nasal process (eFig. 2-5A). The mesenchyme of the fronto-nasal process, a conspicuous swelling over the developing forebrain vesicles, arises from the neural crest and does not appear to have any association with pharyngeal arch development. The fronto-nasal process is innervated by the ophthalmic division of the trigeminal nerve and forms the tissues above the eye as far back as the vertex, thus explaining the sensory cutaneous distribution in the adult. The fronto-nasal process also gives rise to medial and lateral nasal swellings around the nasal pits (eFig. 2-5B). The maxillary processes grow medially beneath the developing eyes and form the lower eyelids. Concomitant with this growth, the eyes also move from their position on the lateral aspect of the embryonic head to the front of the face. The *nasolacrimal groove* on each side lies along the line of fusion of the maxillary process with the lateral nasal swelling (eFig. 2-5C). The ectoderm of the groove invaginates (10 mm stage) into the surrounding mesenchyme to form the *nasolacrimal duct*, which at this stage consists of a solid cord of ectodermal cells that grows upwards into the lids to form the canaliculi and downwards into the nose. Canalization of the solid columns of cells commences first in the vicinity of the lacrimal sac (3 months). Mesenchyme condenses and ossifies around this cord of cells to form the bony walls of the nasolacrimal canal.

The upper eyelid develops from the fronto-nasal process and both lids are visible early in the second month (Fig. 2-1E). The primitive lid folds fuse in weeks 9–10 of gestation, enclosing a surface ectoderm-lined cavity, the conjunctival sac (Fig. 2-2D). Myocytes differentiate in the mesenchyme of both lids and eventually form the orbicularis oculi muscle (second arch derived – nerve supply, facial nerve). Meibomian glands, sebaceous glands and eyelashes develop as invaginations of the conjunctival epithelium or epidermis and are therefore ectodermal derivatives. In the seventh week the future *lacrimal gland* arises as a bud of epithelial cells from the region of the upper temporal conjunctiva sac.

At birth and in the infant, the eyes in humans are in a comparatively advanced state of development relative to the rest of the face; the orbits are therefore large, although the remainder of the facial skeleton is small by comparison with the adult. During infancy and childhood, as a consequence of the development of teeth and growth of the

paranasal sinuses, the facial skeleton steadily increases in size relative to the neurocranium. With the exception of the frontal sinuses, the paranasal sinuses develop as diverticulae from the nasal passages around the fifth month of gestation and are rudimentary at birth. The frontal sinuses appear in the fifth to sixth postnatal year as evaginations from the ethmoid sinuses or middle meatus.

CONGENITAL MALFORMATIONS

Classification of congenital malformations or abnormalities is difficult for several reasons. First, the aetiology is often unknown and, even where a single genetic or environmental cause is suspected, it is often difficult to ascribe full responsibility to such agents or events because exposure to widely different teratogenic agents, such as drugs or trauma, can result in identical developmental defects. Second, defects may be strongly associated with chromosomal abnormality (e.g. trisomy 13).

Furthermore, disturbances in basic cellular events such as neural tube closure may lead to multisystem pathologies. In common with more generalized developmental defects, the consequences of exposure to teratogenic agents are highly dependent on the timing of major embryonic or fetal developmental events occurring at the time of exposure: there are important known *periods of vulnerability*, or critical (sensitive) periods, during which morphogenesis of particular systems and organs may be at risk. In this respect the eye is highly vulnerable for a long period of embryonic and fetal development because there are crucial developmental landmarks from the point of formation of the optic pits (day 22) until late in gestation, with such events as retinal vascularization and pupillary membrane regression occurring close to birth.

Congenital malformations affecting ocular tissues may have the following causes:

Genetic Causes

- *Chromosomal anomalies*: deletions (*cri-du-chat* syndrome, Turner syndrome), trisomies (trisomy 13 or Patau syndrome, Down syndrome, Klinefelter syndrome) and triploidy (see Table 2-1)
- *Hereditary*: either sporadic mutations (aniridia with Wilms' tumour) or dominant/recessive inheritance.

Environmental Causes

- *Drugs*: alcohol, tobacco, anticonvulsants, thalidomide
- *Vitamins and minerals*: excess (e.g. hypervitaminosis A) or deficiency (e.g. folic acid, zinc)
- *Infection*: e.g. rubella, syphilis, toxoplasmosis
- *Radiation*: X-rays.

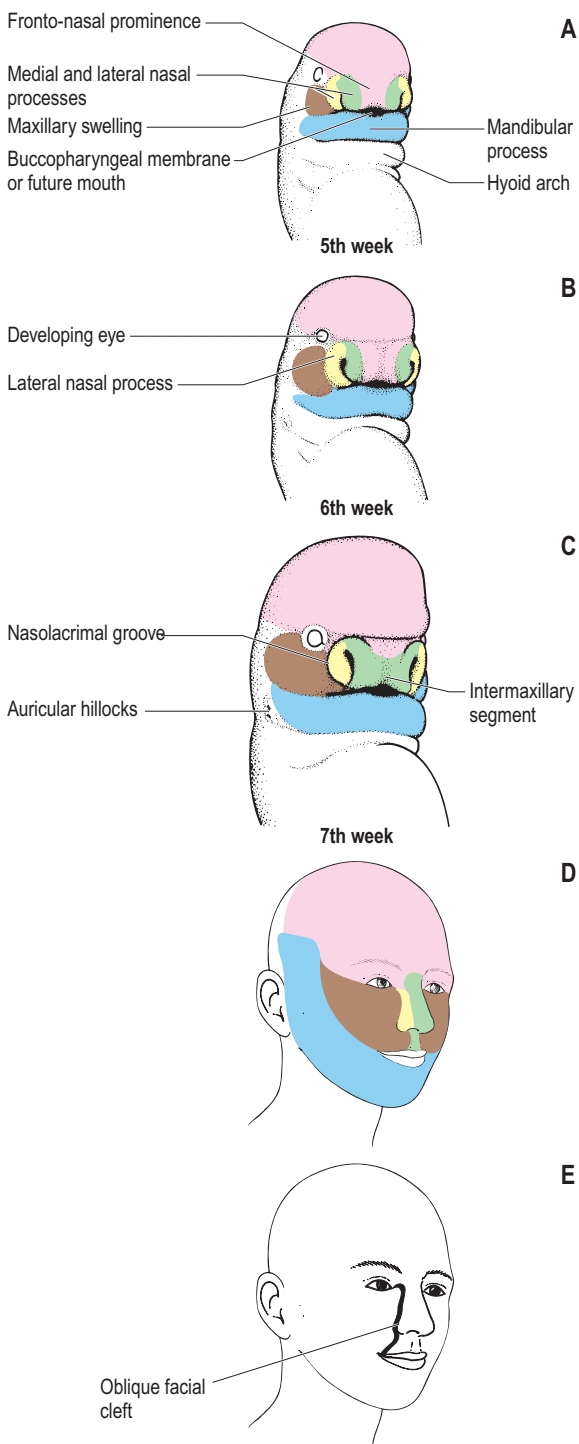
Maternal Age

There is an increased incidence of genetic abnormalities in the oocyte with advancing maternal age.

eBox 2-3**Craniofacial abnormalities**

Skeletal development can be considered to have three essential steps: (1) classic induction (as the result of mesenchyme–epithelium interactions mediated by highly conserved signalling molecules such as Bmp (bone morphogenetic protein) and FGF (fibroblast growth factor)); (2) condensation of mesenchyme; and (3) overt differentiation. Interestingly, 65% of skeletal abnormalities of the head and neck are the result of defects in this first signalling step (Hall, 1998).

It is now recognized that a group of craniofacial abnormalities, the mandibulofacial dysostoses, including Treacher Collins and Hallerman–Streiff syndromes, are caused by deficits in neural crest cell migration and differentiation in the first and second pharyngeal arches. These are manifest as abnormal ear development, hypoplasia of the maxilla and mandible, and lower lid defects. These and more generalized disturbances of neural crest migration, e.g. Rieger syndrome, Pierre Robin syndrome, and conditions affecting primarily the periorbital region such as Peters' anomaly, are increasingly being classified as *neurocristopathies* because of their proposed link to disturbances in neural crest cell migration, proliferation and differentiation.



eFIGURE 2-5 Early development of the face (A–C), the adult form (D), and one of the many congenital abnormalities, oblique facial cleft (E), that results from incomplete fusion of the facial swellings.

eBox 2-4***Developmental anomalies of the nasolacrimal duct***

Disturbances in morphogenetic processes may lead to multiple canaliculi and punctae, abnormal diverticulae, and blockage of the nasolacrimal duct, possibly because of debris from the degenerating central cells producing a mucocoele (not uncommon in the first few weeks after birth).

There is a range of *congenital facial defects*, of which cleft lip and palate are the most common. These are a consequence of complete or partial failure of fusion of the various processes and swellings in the face. Oblique facial clefts occur along the course of the nasolacrimal duct (eFig. 2-5E). The aetiology of these conditions is multifactorial, although maternal exposure to anticonvulsant drugs (phenytoin) and vitamin A are known teratogenic agents that produce these defects. The spatial and temporal expression of retinoic acid receptors during embryological development is currently the subject of much research. While details are still emerging, it is clear that the patterns of expression partially explain the effects of retinoic acid (a vitamin A derivative) as a potent morphogen. Retinoic acid appears sequentially to activate genes of the *Hox* cluster, thereby influencing the normal segmental pattern of hindbrain development (rhombomeres), neural crest migration pathways into pharyngeal arches, and development of the face (Maden et al., 1992).

eBox 2-5***Trisomy 13 (Patau syndrome)***

The ocular pathology in trisomy 13 illustrates various forms of malformation. The cornea and chamber angle are malformed and persistent hyperplastic primary vitreous is common. An anterior coloboma is present and is characterized by a fibrous ingrowth that contains nodules of cartilage. Retinal dysplasia is extensive. Optic nerve malformation is limited to hypoplasia. The systemic malformations are not compatible with survival and are extreme forms of brain malformation (arrhinencephaly) with cardiac and renal malformation.

eBox 2-6***Trisomy 21 (Down syndrome)***

The systemic disturbances in this disorder are well known. In ophthalmology the important components are a high incidence of keratoconus and cataract. Small nodules are formed by spindle cells on the iris (Brushfield's spots); myopia and the attendant complication of retinal detachment may require surgical intervention.

FURTHER READING

- Bartelmez, G.W., Blount, M.P., Gage, P.J., Rhoades, W., Prucka, S.K., Hjalt, T., 1954. The formation of neural crest from the primary optic vesicle in man. *Contr. Embryol.* 35, 55–71.
- Blankenship, T., Peterson, P.E., Hendricks, A.G., 1996. Emigration of neural crest cells from macaque optic vesicles is correlated with discontinuities in its basement membrane. *J. Anat.* 188, 473–483.
- Bohnsack, B.L., Gallina, D., Thompson, H., Kasprick, D.S., Lucarelli, M.J., Dootz, G., et al., 2011. Development of extraocular muscles requires early signals from periocular neural crest and the developing eye. *Arch. Ophthalmol.* 129, 1030–1041.
- Chan-Ling, T., 1997. Glial, vascular, and neuronal cytogenesis in whole-mounted cat retina. *Microsc. Res. Tech.* 36, 1–16.
- Chauhan, B.K., Disanza, A., Choi, S.Y., Faber, S.C., Lou, M., Beggs, H.E., et al., 2009. Cdc42- and IRSp53-dependent contractile filopodia tether presumptive lens and retina to coordinate epithelial invagination. *Development* 136, 3657–3667.
- Collinson, J.M., Hill, R.E., West, J., 2004. Analysis of mouse eye development with chimeras and mosaics. *Int. J. Dev. Biol.* 48, 793–804.
- Creuzet, S., Vincent, C., Couly, G., 2005. Neural crest derivatives in ocular and periocular structures. *Int. J. Dev. Biol.* 49, 161–171.
- Cvekl, A., Tamm, E.R., 2004. Anterior eye development and ocular mesenchyme: new insights from mouse models and human diseases. *Bioessays* 26, 374–386.
- Erickson, C.A., Loring, J.F., Lester, S.M., 1989. Migratory pathways of HNK-1-immunoreactive neural crest cells in the rat embryo. *Dev. Biol.* 134, 112–118.
- Fukiishi, Y., Morriss-Kay, G.M., 1992. Migration of neural crest cells to the pharyngeal arches and heart in rat embryos. *Cell Tissue Res.* 268, 1–8.
- Gage, P.J., Rhoades, W., Prucka, S.K., Hjalt, T., 2005. Fate maps of neural crest and mesoderm in the mammalian eye. *Invest. Ophthalmol. Vis. Sci.* 46, 4200–4208.
- Gilland, E., Baker, R., 1993. Conservation of neuroepithelial and mesodermal segments in the embryonic vertebrate head. *Acta Anat.* 148, 110–123.
- Hall, B.K., 1998. Evolutionary developmental biology. Kluwer Academic Publishers, Dordrecht.
- Hall, B.K., 2005. Bones and cartilage: developmental and evolutionary skeletal biology. Elsevier Academic Press, London.
- Heavner, W., Pevny, L., 2012. Eye development and retinogenesis. *Cold Spring Harb. Perspect. Biol.* 4, pii: a008391.
- Hunt, P., Wilkinson, D., Krumlauf, R., 1991. Patterning the vertebrate head: murine *Hox2* genes mark distinct subpopulations of premigratory and migratory cranial neural crest. *Development* 112, 43–50.
- Lang, R.A., 2004. Pathways regulating lens induction in the mouse. *Int. J. Dev. Biol.* 48, 783–791.
- Lang, R.A., Bishop, J.M., 1993. Macrophages are required for cell death and tissue remodelling in the developing mouse eye. *Cell* 74, 453–462.
- Larsen, W.J., 1997. Human embryology, second ed. Churchill Livingstone, New York.
- Maden, M., Horton, C., Graham, A., Leonard, L., Pizzey, J., Siegenthaler, G., et al., 1992. Domains of cellular retinoic acid-binding protein I (CRABP I) expression in the hindbrain and neural crest of the mouse embryo. *Mech. Dev.* 37, 13–23.
- Mann, I., 1928. The development of the human eye. Grune and Stratton, New York.
- Mann, I., 1964. The development of the human eye, third ed. Grune and Stratton, New York.
- Matsuoka, T., Ahlberg, P.E., Kessaris, N., Iannarelli, P., Dennehy, U., Richardson, W.D., et al., 2005. Neural crest origins of the neck and shoulder. *Nature* 436, 347–355.
- McAvoy, J.W., Chamberlain, C.G., de Jongh, R.U., 1999. Lens development. *Eye* 13, 425–437.
- McMenamin, P.G., 1989. A morphological study of the inner surface of the anterior chamber angle in pre- and post-natal human eyes. *Curr. Eye Res.* 8, 727–739.
- McMenamin, P.G., 1989. The human foetal iridocorneal angle: a scanning electron microscopic study. *Br. J. Ophthalmol.* 73, 871–879.
- McMenamin, P.G., 1991. A quantitative study of the prenatal development of aqueous outflow system in the human eye. *Exp. Eye Res.* 53, 507–517.
- McMenamin, P.G., Djano, J., Wealthall, R., Griffin, B.J., 2002. Characterisation of the macrophages associated with the tunica vasculosa lentis of the rat eye. *Invest. Ophthalmol. Vis. Sci.* 43, 2076–2082.
- McMenamin, P.G., Krause, W., 1993. Development of the eye in the North American opossum (*Didelphis virginiana*). *J. Anat.* 183, 343–358.
- Mendelson, C., Larkin, S., Mark, M., LeMeur, M., Clifford, J., Zelent, A., et al., 1994. RAR β isoforms: distinct transcriptional control by retinoic acid and specific spatial patterns of promotor activity during mouse embryonic development. *Mech. Dev.* 45, 227–241.
- Monaghan, A.P., Davidson, D.R., Sime, C., 1991. The Msh-like homeobox genes define domains in the developing vertebrate eye. *Development* 112, 1053–1061.
- Noden, D., 1982. Periocular mesenchyme: neural crest and mesoderm interactions. In: Jakobiec, F.A. (Ed.), *Ocular anatomy, embryology and teratology*. Harper and Row, Philadelphia, pp. 97–119.
- Noden, D.M., 1988. Interactions and fate of avian craniofacial mesenchyme. *Development* 103 (Suppl.), 121–140.
- Noden, D.M., 1991. Vertebrate craniofacial development: the relation between ontogenetic process and morphological outcome. *Brain Behav. Evol.* 38, 190–225.
- O'Rahilly, R., 1966. The prenatal development of the human eye. *Exp. Eye Res.* 21, 93–112.
- Osumi-Yamashita, N.O., Noji, S., Nohno, T., Koyama, E., Doi, H., Eto, K., et al., 1990. Expression of retinoic acid receptor genes in neural crest-derived cells during mouse facial development. *FEBS Lett.* 264, 71–74.
- Ozanics, V., Jakobiec, F.A., 1982. Prenatal development of the eye and its adnexa. In: Jakobiec, F.A. (Ed.), *Ocular anatomy, embryology and teratology*. Harper and Row, Philadelphia, pp. 11–96.
- Patapoutian, A., Miner, J., Lyons, G.E., Wold, B., 1993. Isolated sequences from the linked *Myf-5* and *MRF4* genes drive distinct patterns of muscle-specific expression in transgenic mice. *Development* 118, 61–69.
- Reese, B.E., Necessary, B.D., Tam, P.P.L., Faulkner-Jones, B., Tan, S.S., 1999. Clonal expansion and cell dispersion in the developing mouse retina. *Eur. J. Neurosci.* 11, 2965–2978.
- Robinson, S.R., 1991. Development of the mammalian retina. In: Dreher, B., Robinson, S.R. (Eds.), *Neuroanatomy of the visual pathways and their development; Cronly-Dillon JR, series ed. Vision and visual dysfunction, vol. 3*. Macmillan, Basingstoke, pp. 69–128.

129.e8 2 Embryology and early development of the eye and adnexa

- Saha, M.S., Spann, C., Grainger, R.M., 1989. Embryonic lens induction: more than meets the optic vesicle. *Cell Differ. Dev.* 28, 153–171.
- Saint-Geniez, M., D'Amore, P., 2004. Development and pathology of the hyaloid, choroidal and retinal vasculature. *Int. J. Dev. Biol.* 48, 1045–1058.
- Schulz, M.W., Chamberlain, C.G., de Longh, R.U., McAvoy, J.W., 1993. Acidic and basic FGF in ocular media and lens: implications for lens polarity and growth patterns. *Development* 118, 117–126.
- Spaeth, G., Nelson, L.B., Beaudoin, A.R., 1982. Ocular teratology. In: Jakobiec, F.A. (Ed.), *Ocular anatomy, embryology and teratology*. Harper and Row, Philadelphia, pp. 955–1080.
- Sullivan, C.H., Braunstein, L., Hazard-Leonards, R.M., Holen, A.L., Samaha, F., Stephens, L., et al., 2004. A re-examination of lens induction in chicken embryos: in vitro studies of early tissue interactions. *Int. J. Dev. Biol.* 48, 771–782.
- Trainor, P.A., Tam, P.P.L., 1995. Cranial paraxial mesoderm and neural crest cells of the mouse embryo: co-distribution in the craniofacial mesenchyme but distinct segregation in the branchial arches. *Development* 121, 2569–2582.
- Zieske, J.D., 2004. Corneal development associated with eyelid opening. *Int. J. Dev. Biol.* 48, 903–911.